Electronic Supplementary Material (ESI) for ChemComm.

Electronic Supplementary Information to:

β-Oxochlorin cobalt(II) complexes catalyze the electrochemical reduction of CO_2

John Nganga, Nivedita Chaudhri,
Christian Brückner,* and Alfredo M. Angeles-Boza*

Department of Chemistry
University of Connecticut
Storrs, CT 06269-3060
Unites States

* Corresponding authors:
alfredo.angeles-boza@uconn.edu, +1-860-486-6718

christian.bruckner@uconn.edu, +1-860-486-2743

ESI Table of Contents

Experimental Section

Materials. Free-base oxochlorin **2**, dioxobacteriochlorins **3**, **4**, and dioxoisobacteriochlorins **5-7**, and trioxopyrrocorphins **8** and **9** were prepared by H_2SO_4/H_2O_2 oxidation of 2,3,7,8,12,13,17,18-octaethylporphyrin (OEP), as described in the literature. The solvents used in the present work were of analytical grade and used without further purification. $CoCl_2 \cdot 6H_2O$, NaOAc, and Li_2CO_3 were purchased from Sigma Aldrich and used as received. Silica gel 60 aluminum baked (250 µm) analytical TLC plate, 500 µm or 1 mm silica gel 60 on glass (20 × 20 cm) preparative TLC plates, and silica gel for column chromatography (premium grade, 60 Å, 40-75 µm) were provided by Sorbent Technologies, Atlanta, GA.

Instruments. UV-vis spectra were recorded on Varian Cary 100 Bio spectrometer using CH_2Cl_2 as solvent. IR spectra were obtained from solid materials on a Bruker Alpha FTIR spectrometer using an attenuated total reflection (ATR) setup (diamond). High resolution ESI mass spectra were recorded using AB Sciex QStar Elite Quadrupole-TOF MS instrument from CH_3CN solution (~10^{-6} M) in positive ion mode. Electrochemical experiments were performed by using a Model 6012D Electrochemical analyzer from CH Instruments, Inc. The head space gas analysis was then accomplished using a SHIMADZU GC2014 gas chromatograph equipped with 60/80 CARBOXEN-1000 15′ x1/8″ SS (2.1 mm I.D.) column. ^{1}H NMR spectra were collected using a Bruker 400 MHz NMR spectrophotometer

Cyclic Voltammetry. Cyclic voltammetry experiments were performed under $N_{2(g)}$ or $CO_{2(g)}$ in a 15mL cell with a three-electrode setup comprised of a glassy carbon working electrode (GCE, 3.0 mm diameter, CHI Instruments), a platinum wire counter electrode and a $Ag/AgNO_3$ reference electrode with ferrocene as an internal reference. All experiments were performed by using 0.1 M tetrabutylammonium hexafluorophosphate ($TBAPF_6$) as the supporting electrolyte, acetonitrile as the solvent, and with analyte concentration of 1.0 mM. During the electrochemical runs an air free headspace of the electrochemical setup was maintained by continuously purging the headspace with either N_2(g) or CO_2(g) via a cannula needle.

In the CV experiments under CO_2, the selection of i_{CO2} was done at the peak catalytic current. The i_{CO2}/i_{N2} ratio has been used in the literature to quantify systems that do not have catalytic responses under pure kinetic control.[2] Since the representation of catalytic activity with i_{CO2}/i_{N2} ratio is not adequate for catalytic work as it involves generation of multi-electron products, our analysis of catalytic activity also used the results obtained from controlled potential electrolysis studies. Reported $E_{cat/2}$ values correspond to half the catalytic peak current.

Controlled Potential Electrolysis: Controlled potential electrolysis studies of the porphyrinoid cobalt(II) complexes were carried out in CH_3CN and at a potential of -2.9V vs the Fc^+/Fc couple. CPE studies were performed in a specialized three compartment cell using a three-electrode set-up which consisting of a glassy carbon rod, a $Ag/AgNO_3$ reference electrode and a platinum wire counter electrode. The solution was saturated with CO_2 for 30 minutes after which it was made airtight and then bulk electrolysis initiated. CPE studies were performed in triplicate unless indicated. The reported TONs were obtained from the controlled potential electrolysis experiments and were estimated by dividing by total amount of catalyst present in bulk solution.

Product Analyses: The gaseous products were then analyzed by sampling the headspace of the electrolysis cell using a gas-tight Hamilton 1001 SL SYR, syringe at the conclusion of electrochemical runs. For the $^{13}CO_2$ studies the mixture in the specialized three compartment cell containing was connected to a Schlenk line and then degassed using freeze-pump-thaw cycles. Special care was taken to ensure that the ground-glass joints were adequately greased to ensure an air-tight seal and prevent air leakage. Thereafter the solution was charged with$^{13}CO_2$. Formate ($HCOO^-$) was analyzed using ^1H NMR techniques.[3] Briefly, post-controlled potential electrolysis solutions that were run without an acid additive were acidified using dilute TFE (0.05 M). However post-CPE solutions that had a TFE previously as an additive were used as such.

Thereafter a sample of 600 μL of the resulting solution was taken into a syringe and added to a 10 mL vial which was then was diluted with 800 μL of CD_3CN. The solution was then sonicated for 10 minutes and then spectra were collected on a 400 MHz NMR Bruker spectrometer using 128 scans and solvent suppression. The amount of formate peak was then quantified using a calibration curve obtained via the analysis of known amounts of formate (0.0 mM, 0.01 mM, 0.05 mM, 0.1 mM, 0.5 mM, 1.0 mM, 5 mM, and 10.0 mM solutions) using an internal standard of dimethyl sulfone in a solvent of D_2O. Further analysis of labeled gaseous products arising from labeled $^{13}CO_2$ substrate was carried out by a Hewlett Packard 5971 mass series selective detector.

References

(1) H. H. Inhoffen and W. Nolte, *Liebigs Ann. Chem.*, **1969**, *725*, 167–176.

(2) M. R. Crawley, K. J. Kadassery, A. N. Oldacre, A. E. Friedman, D. C. Lacy, T. R. Cook, *Organometallics* **2019**, *38*, 1664–1676.

(3) Y. Hameed, B. Gabidullin, D. Richeson, *Inorg. Chem*. **2018**, *57*, 13092–13096.

General Synthetic Procedure for the Synthesis of the Oxochlorin Cobalt(II) Complexes[1]

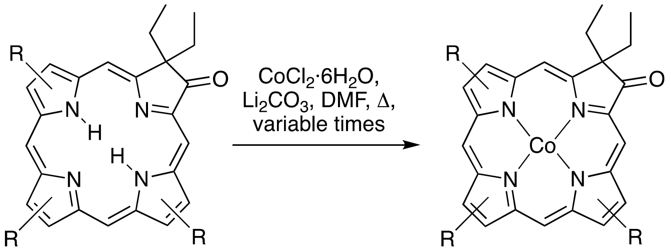

Free base (40 mg) oxochlorins, $CoCl_2·6H_2O$ (5.0 equiv.), and Li_2CO_3 (3.0 equiv.) were dissolved in DMF (20 mL) and heated to reflux and the progress of the reaction was monitored by thin layer chromatography. Oxochlorin (**2**), isobacteriochlorins (**3**, **4**, and **5**), and pyrrocorphins (**8** and **9**) took less time (35-40 min) for completion as compared to the bacteriochlorins (**6** and **7**) (3.5-4 h). After completion of the reaction, the reaction mixture was cooled to ambient temperature and the complexes were precipitated by slow addition of deionized water (~100 mL). The precipitate was isolated by microfiltration. The crude cobalt hydroporphyrins were dissolved in the minimum amount of CH_2Cl_2 and purified by column chromatography (silica, hexanes/CH_2Cl_2 (1:1 v/v), followed by 100% CH_2Cl_2).

---

[1] Generalized procedure adopted from: D. Schnable, N. Chaudhri, R. Li, M. Zeller and C. Brückner, *Inorg. Chem.*, 2020, **59**, 2870−2880.

[Octaethyl-7-oxo-chlorinato]cobalt(II) (2Co)

Prepared in 93% yield (41.0 mg, 6.75 × 10^{-5} M) according to the general procedure: MW = 607.69 g/mol; R_f = 0.73 (silica-CH_2Cl_2); UV-vis (CH_2Cl_2) λ_{max} (log ε): 321 (4.19), 369 (4.47), 410 (4.88), 568 (3.82), 616 (4.42) nm; HR-MS (ESI+, 100% CH_3CN, TOF): *m/z* calc'd for $C_{36}H_{44}N_4OCo$ 607.2847 (for M^+); found: 607.2842.

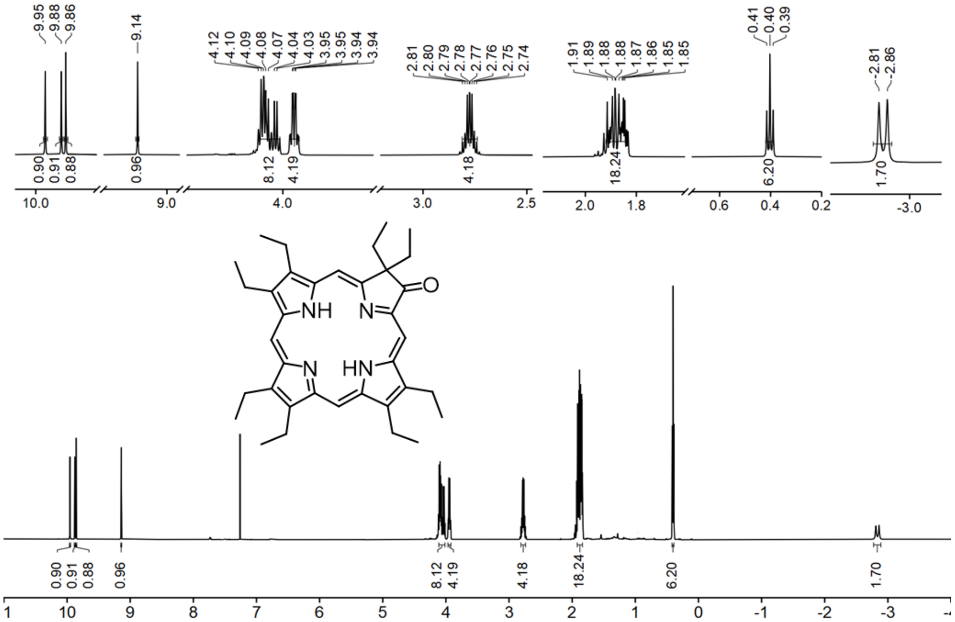

Figure S1. ^{1}H NMR spectrum (600 MHz, $CDCl_3$, 25 °C) of free-base octaethyl-7-oxochlorin (**2**).

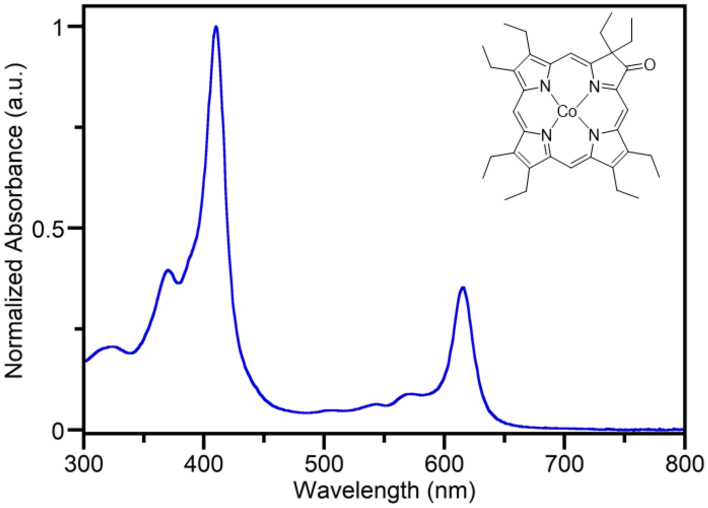

Figure S2. Normalized UV-vis spectrum (CH_2Cl_2) of **2Co**.

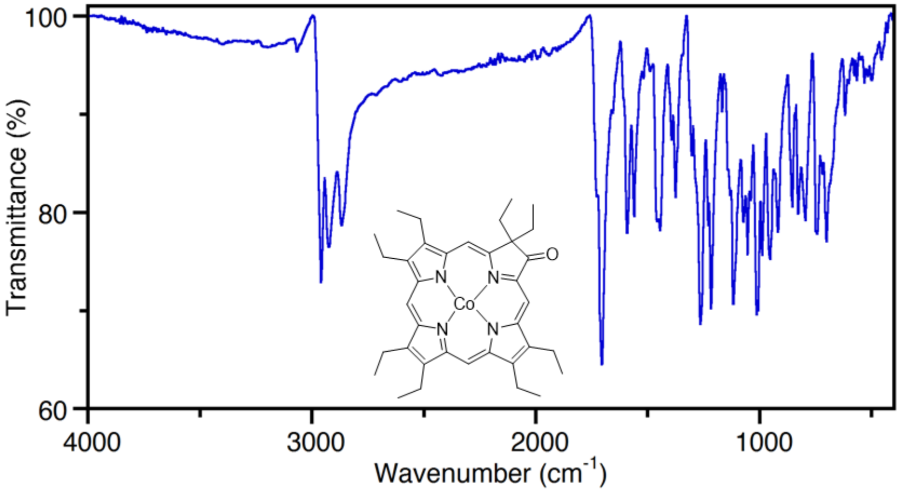

Figure S3. FT-IR spectrum (neat, ATR) of **2Co**.

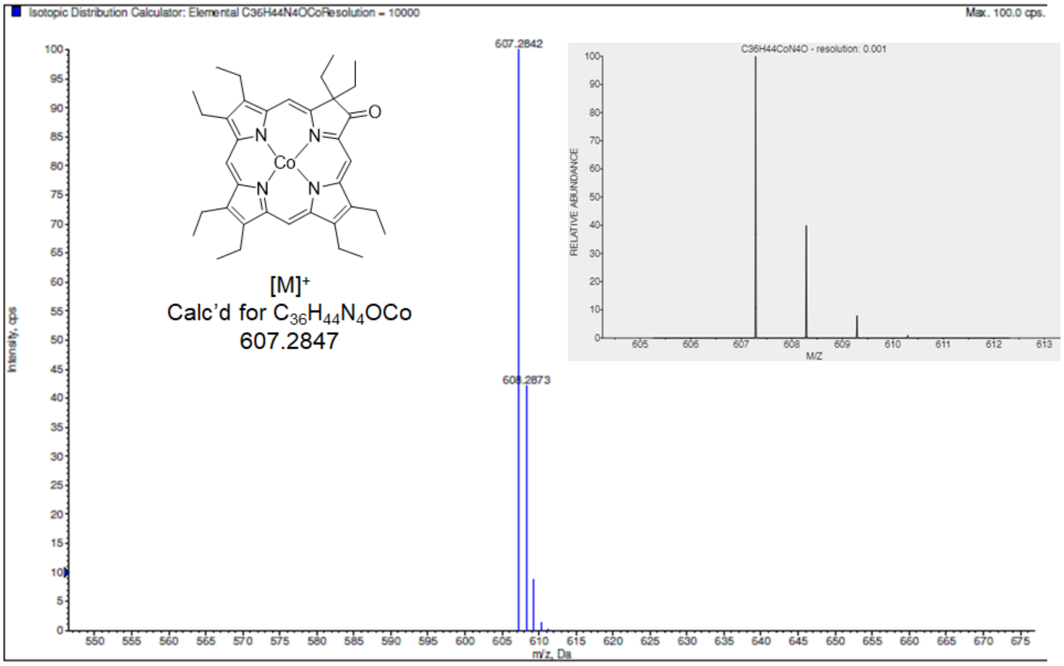

Figure S4. HR-MS (ESI+, 100% CH_3CN, TOF) of **2Co**.

[Octaethyl-7,17-dioxo-bacteriochlorinato]cobalt(II) (3Co)

Prepared in 91% yield (40.0 mg, 6.41 × 10^{-5} M) according to the general procedure: MW = 623.69 g/mol; R_f = 0.30 (silica-CH_2Cl_2); UV-vis (CH_2Cl_2) λ_{max} (log ε): 319 (4.39), 375 (4.44), 421 (4.76), 508 (3.50), 546 (3.38), 635 (3.71), 661 (3.92), 696 (4.92) nm; HR-MS (ESI+, 100% CH_3CN, TOF): *m/z* calc'd for $C_{36}H_{44}N_4O_2Co$ 623.2796 (for M^+); found: 623.2791.

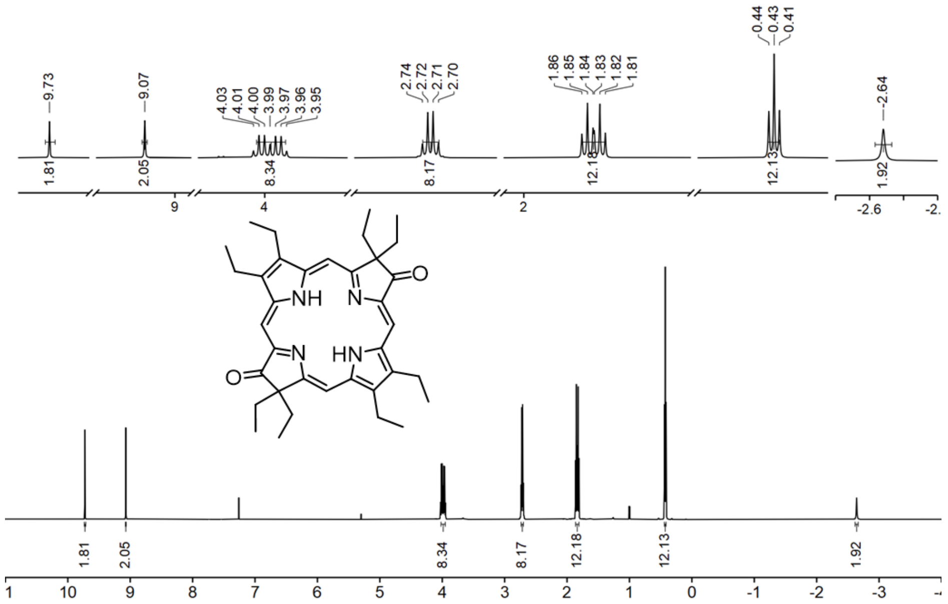

Figure S5. ^{1}H NMR spectrum (600 MHz, $CDCl_3$, 25 °C) of free-base Octaethyl-7,17-dioxo-bacteriochlorin (**3**).

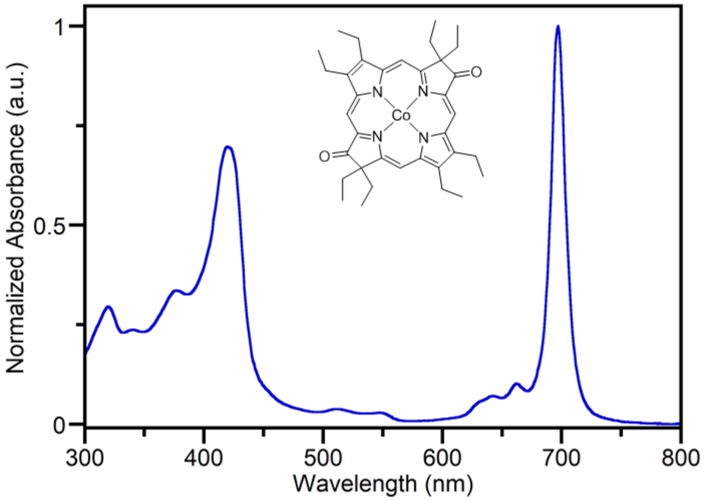

Figure S6. Normalized UV-vis spectrum (CH_2Cl_2) of **3Co**.

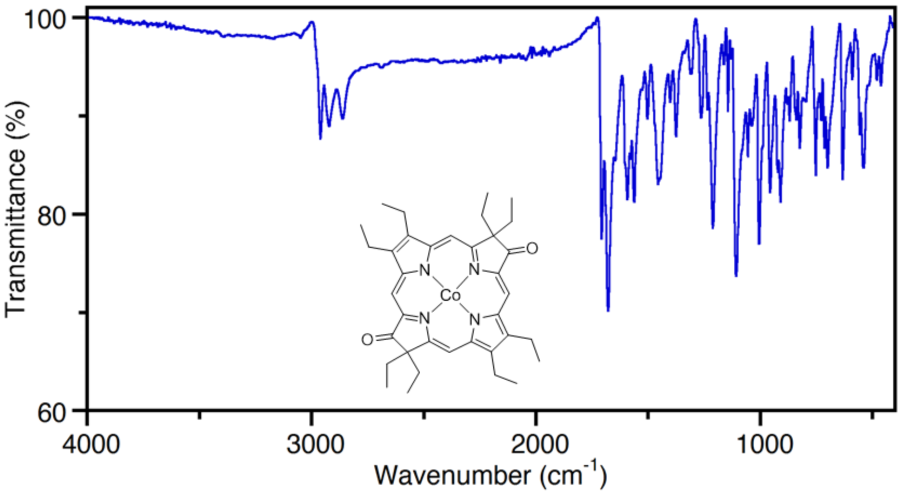

Figure S7. FT-IR spectrum (neat, ATR) of **3Co**.

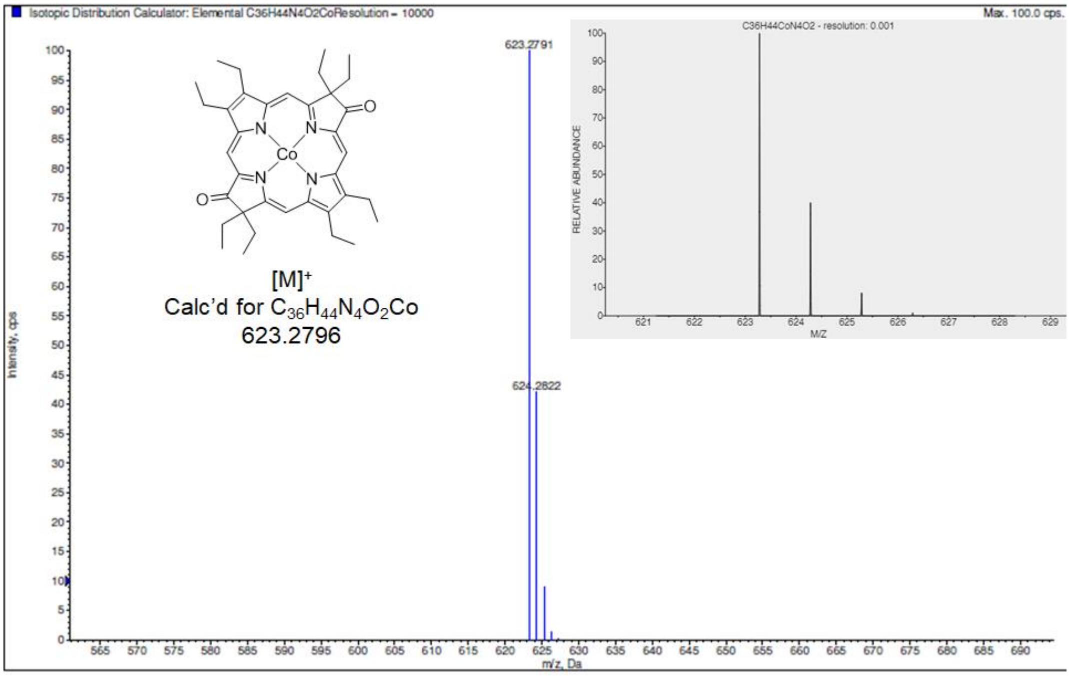

Figure S8. HR-MS (ESI+, 100% CH_3CN, TOF) of **3Co**.

[Octaethyl-7,18-dioxo-bacteriochlorinato]cobalt(II) (4Co)

Prepared in 92% yield (40.5 mg, 6.49 × 10^{-5} M) according to the general procedure: MW = 623.69 g/mol; R_f = 0.23 (silica-CH_2Cl_2); UV-vis (CH_2Cl_2) λ_{max} (log ε): 308 (4.26), 376 (4.37), 422 (4.53), 588 (3.93), 666 (4.42) nm; HR-MS (ESI+, 100% CH_3CN, TOF): *m/z* calc'd for $C_{36}H_{44}N_4O_2Co$ 623.2796 (for M^+); found: 623.2791.

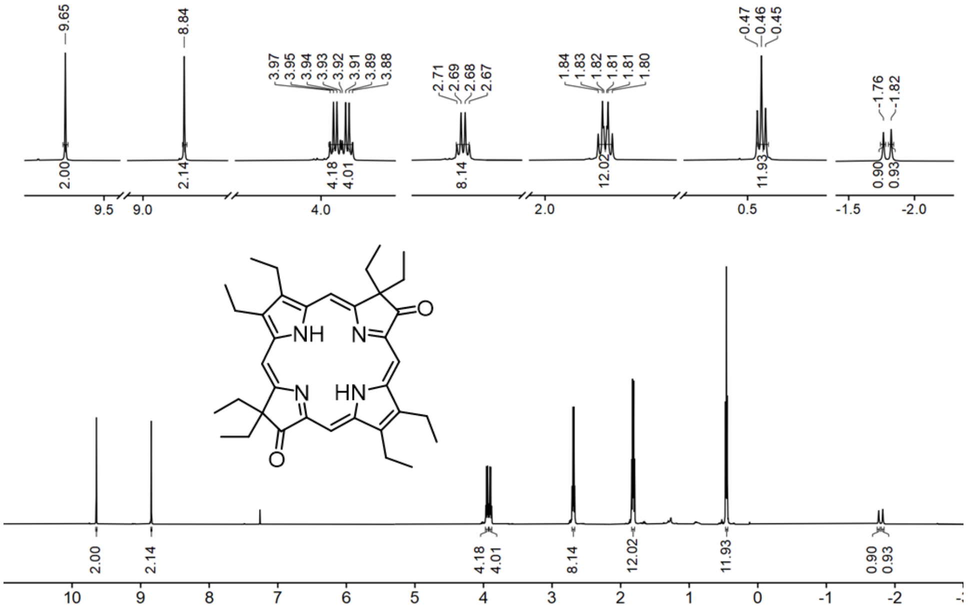

Figure S9. ^{1}H NMR spectrum (600 MHz, $CDCl_3$, 25 °C) of free-base Octaethyl-7,18-dioxo-bacteriochlorin (**4**).

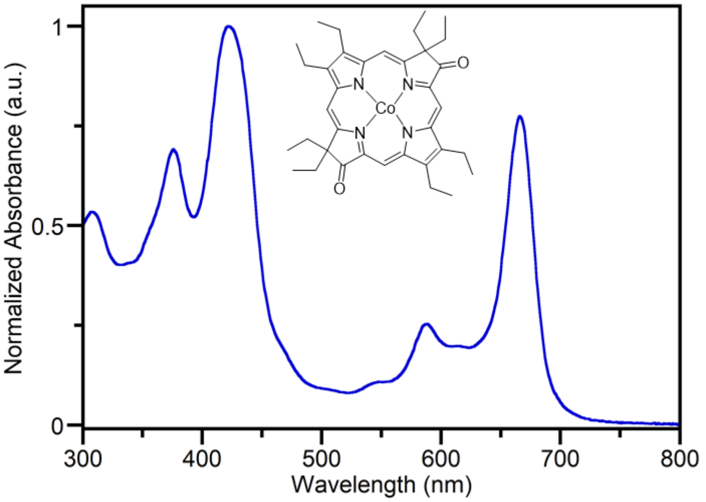

Figure S10. Normalized UV-vis spectrum (CH_2Cl_2) of **4Co**.

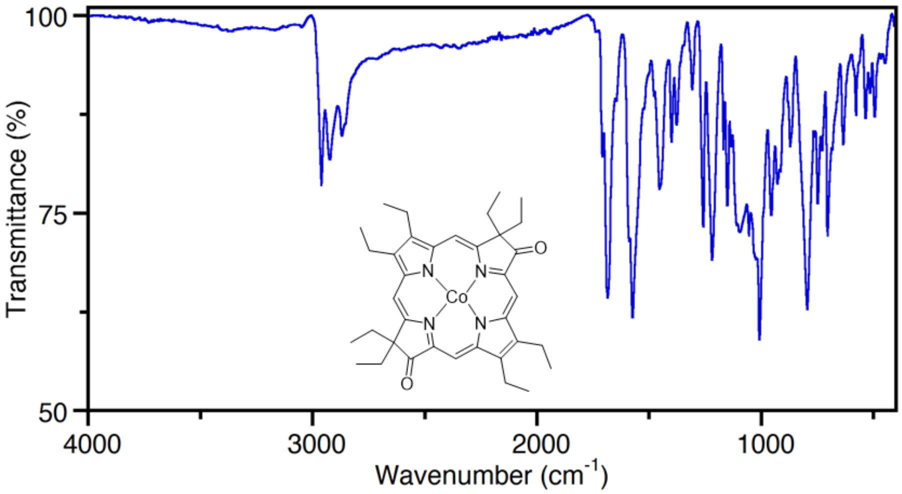

Figure S11. FT-IR spectrum (neat, ATR) of **4Co**.

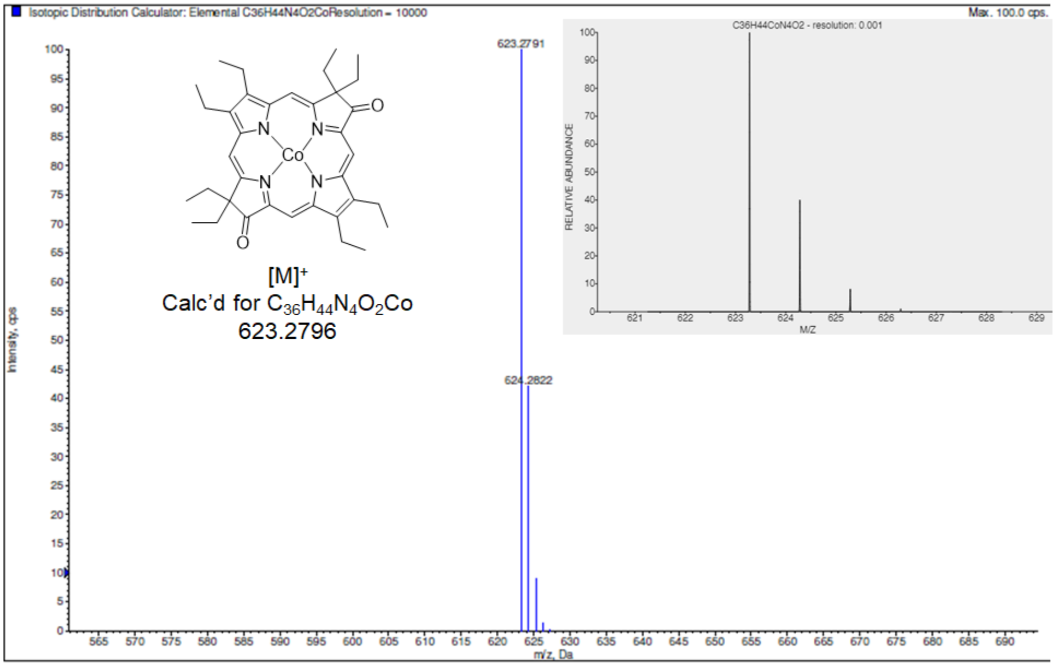

Figure S12. HR-MS (ESI+, 100% CH_3CN, TOF) of **4Co**.

[Octaethyl-2,7-dioxo-isobacteriochlorinato]cobalt(II) (5Co)

Prepared in 96% yield (42.3 mg, 6.78 × 10^{-5} M) according to the general procedure: MW = 623.69 g/mol; R_f = 0.18 (silica-CH_2Cl_2); UV-vis (CH_2Cl_2) λ_{max} (log ε): 388 (4.36), 423 (4.30), 578 (3.80), 620 (4.26) nm; HR-MS (ESI+, 100% CH_3CN, TOF): *m/z* calc'd for $C_{36}H_{44}N_4O_2Co$ 623.2796 (for M^+); found: 623.2791.

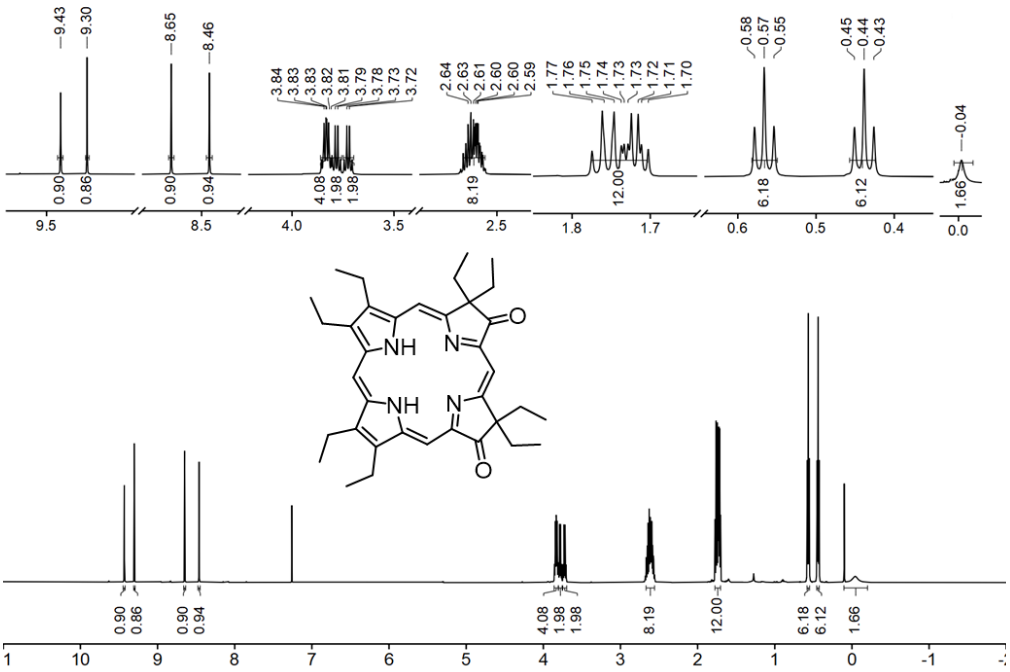

Figure S13. ^{1}H NMR spectrum (600 MHz, $CDCl_3$, 25 °C) of free-base Octaethyl-2,7-dioxo-isobacteriochlorin (**5**).

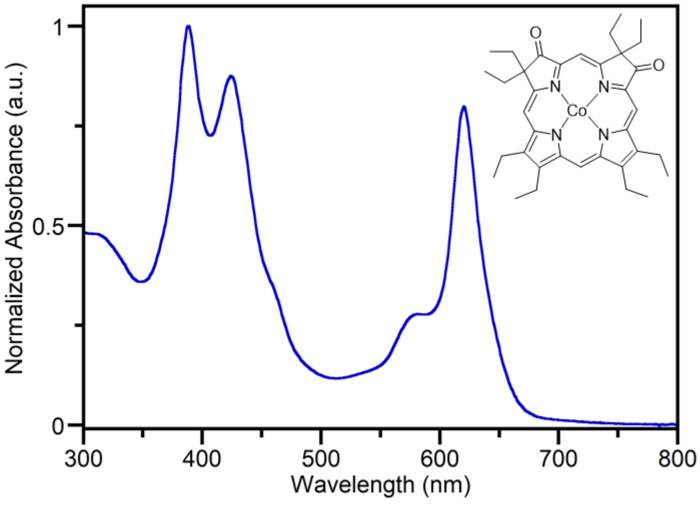

Figure S14. Normalized UV-vis spectrum (CH_2Cl_2) of **5Co**.

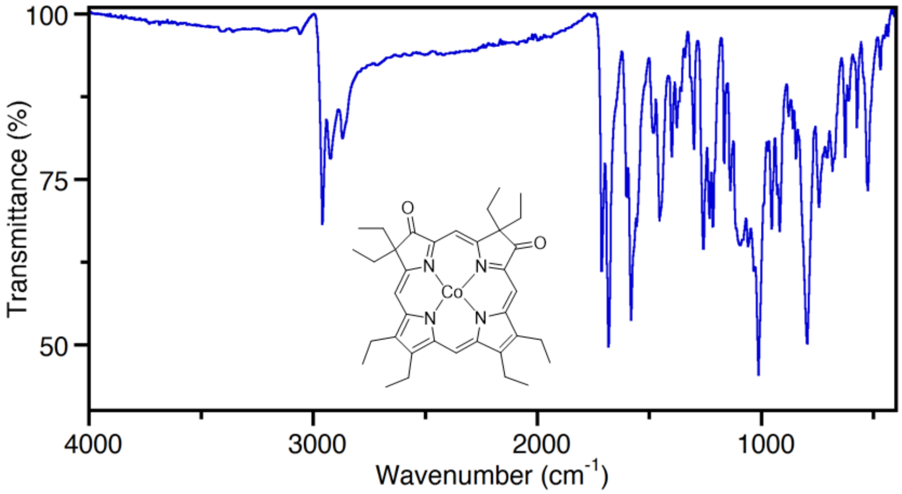

Figure S15. FT-IR spectrum (neat, ATR) of **5Co**.

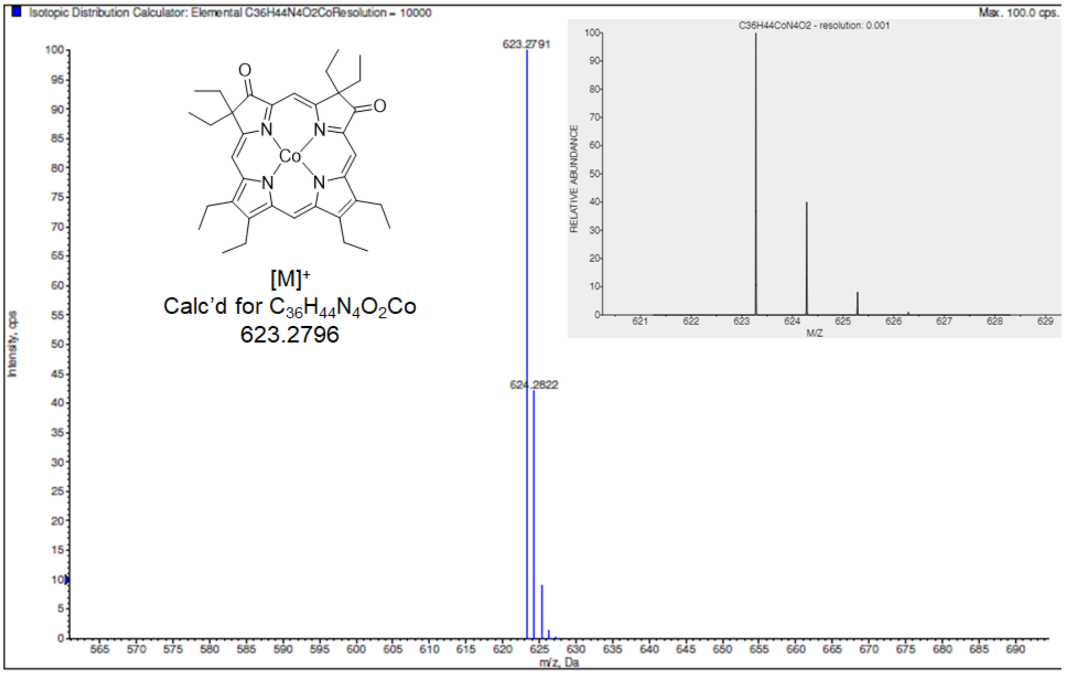

Figure S16. HR-MS (ESI+, 100% CH_3CN, TOF) of **5Co**.

[Octaethyl-3,7-dioxo-isobacteriochlorinato]cobalt(II) (6Co)

Prepared in 94% yield (41.4 mg, 6.63 × 10^{-5} M) according to the general procedure: MW = 623.69 g/mol; R_f = 0.10 (silica-CH_2Cl_2); UV-vis (CH_2Cl_2) λ_{max} (log ε): 319 (4.06), 425 (4.56), 530 (3.47), 567 (3.64), 634 (3.60), 695 (4.38) nm; HR-MS (ESI+, 100% CH_3CN, TOF): *m/z* calc'd for $C_{36}H_{44}N_4O_2Co$ 623.2796 (for M^+); found: 623.2791.

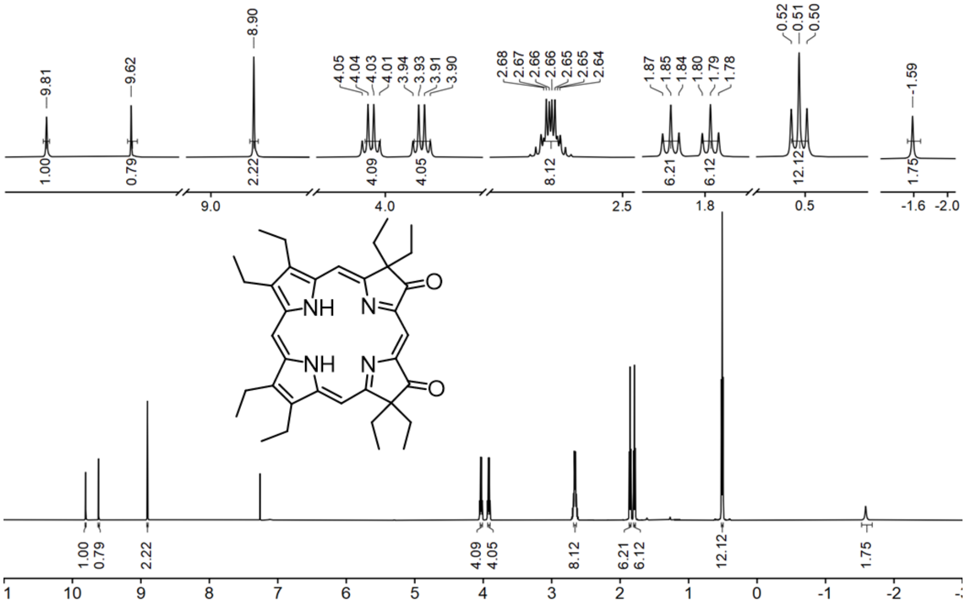

Figure S17. ^{1}H NMR spectrum (600 MHz, $CDCl_3$, 25 °C) of free-base Octaethyl-3,7-dioxo-isobacteriochlorin (**6**).

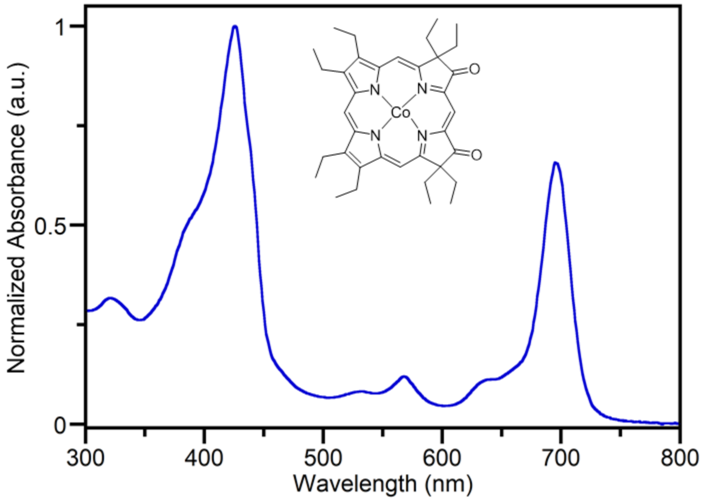

Figure S18. Normalized UV-vis spectrum (CH_2Cl_2) of **6Co**.

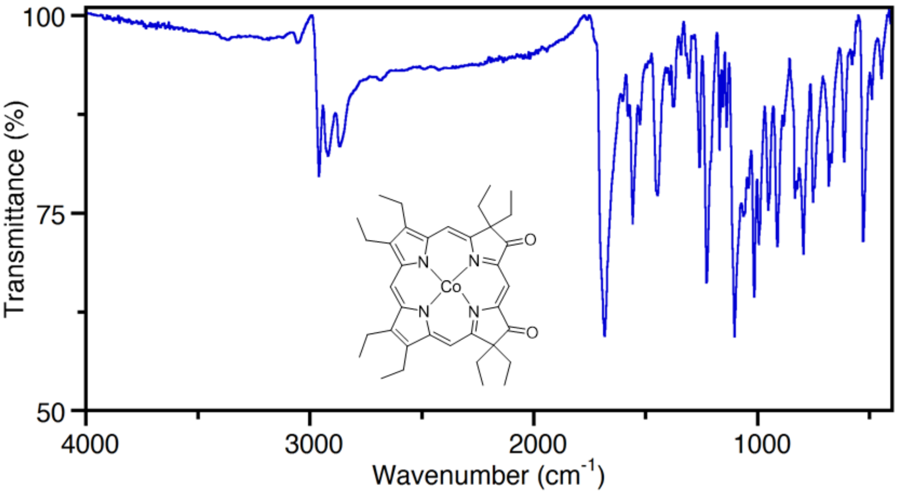

Figure S19. FT-IR spectrum (neat, ATR) of **6Co**.

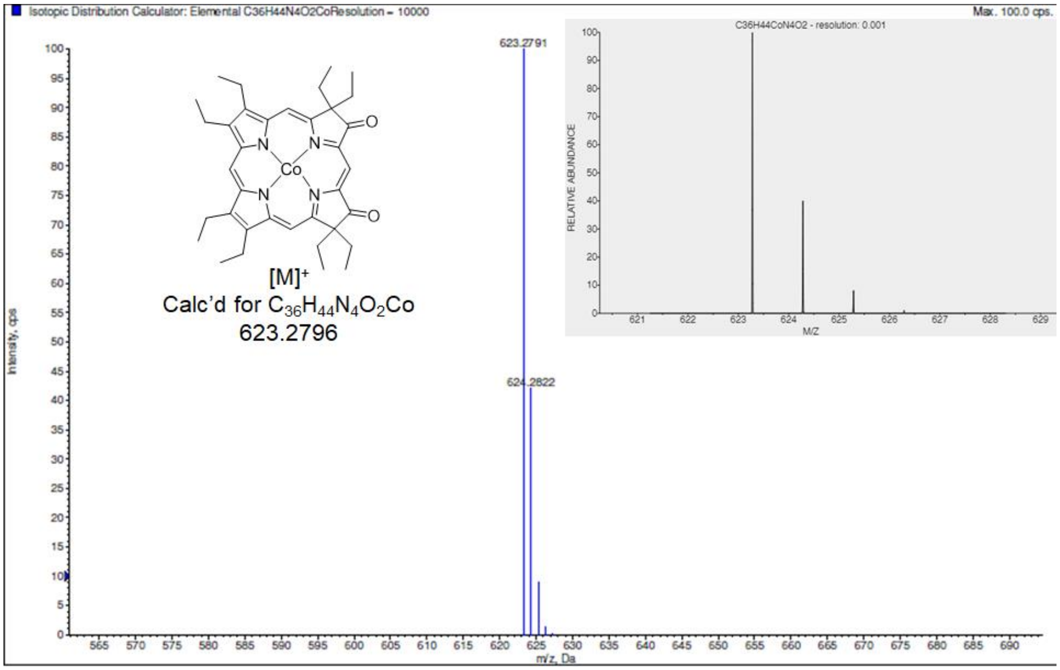

Figure S20. HR-MS (ESI+, 100% CH_3CN, TOF) of **6Co**.

[Octaethyl-7,13-dioxo-isobacteriochlorinato]cobalt(II) (7Co)

Prepared in 93% yield (41.0 mg, 6.56 × 10^{-5} M) according to the general procedure: MW = 623.69 g/mol; R_f = 0.32 (silica-CH_2Cl_2); UV-vis (CH_2Cl_2) λ_{max} (log ε): 320 (4.12), 361 (4.20), 409 (4.48), 598 (3.72), 649 (4.31) nm; HR-MS (ESI+, 100% CH_3CN, TOF): *m/z* calc'd for $C_{36}H_{44}N_4O_2Co$ 623.2796 (for M^+); found: 623.2791.

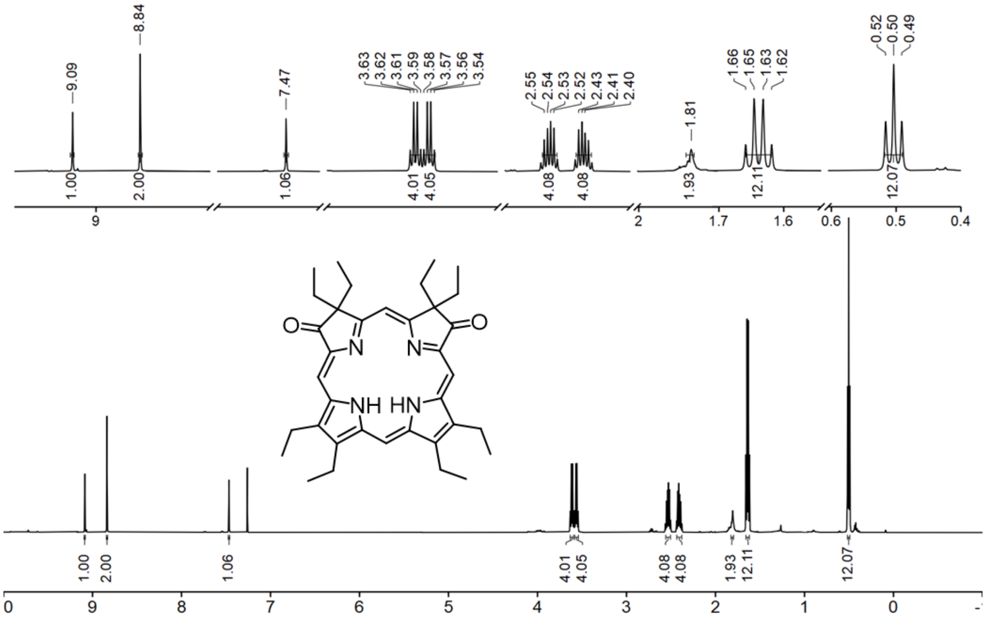

Figure S21. ^{1}H NMR spectrum (600 MHz, $CDCl_3$, 25 °C) of free-base Octaethyl-7,13-dioxo-isobacteriochlorin (**7**).

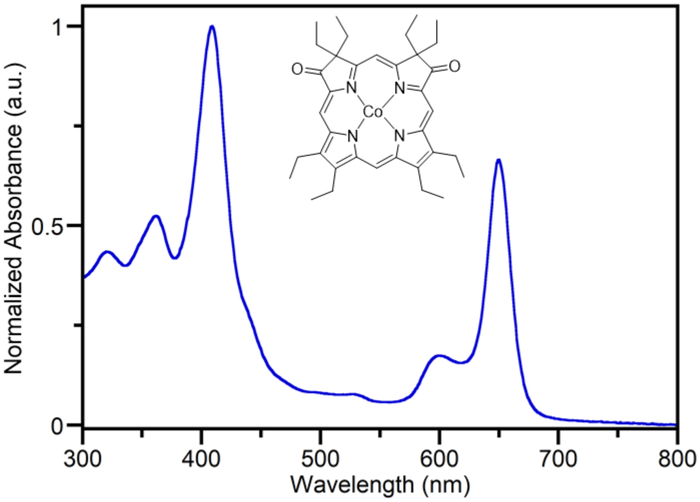

Figure S22. Normalized UV-vis spectrum (CH_2Cl_2) of **7Co**.

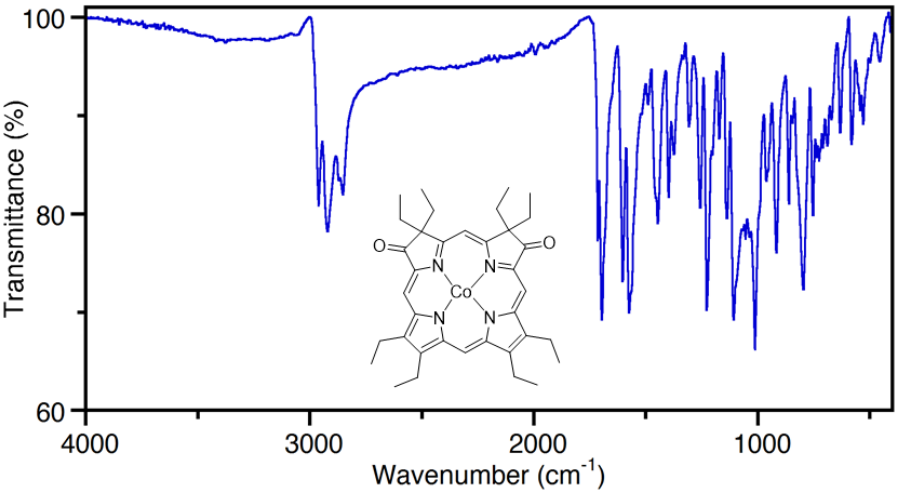

Figure S23. FT-IR spectrum (neat, ATR) of **7Co**.

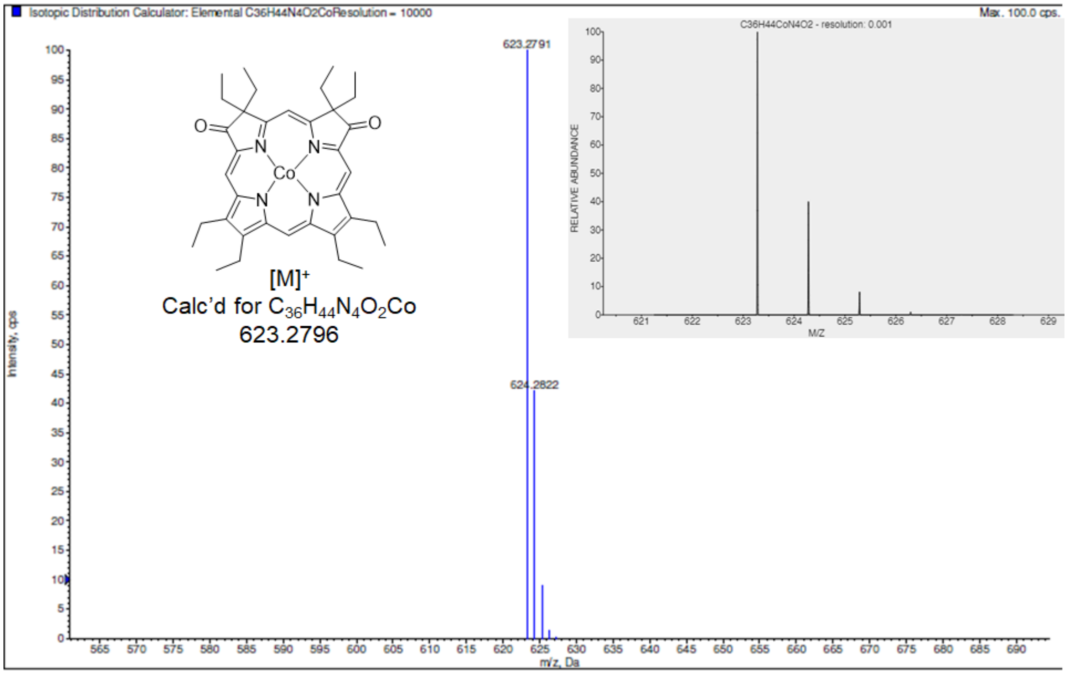

Figure S24. HR-MS (ESI+, 100% CH_3CN, TOF) of **7Co**.

[Octaethyl-2,7,18-trioxo-pyrrocorphinato]cobalt(II) (8Co)

Prepared in 95% yield (41.7 mg, 6.52 × 10^{-5} M) according to the general procedure: MW = 639.69 g/mol; R_f = 0.25 (silica-1% acetone/CH_2Cl_2); UV-vis (CH_2Cl_2) λ_{max} (log ε): 424 (3.93), 675 (3.65), 724 (4.17) nm; HR-MS (ESI+, 100% CH_3CN, TOF): *m/z* calc'd for $C_{36}H_{44}N_4O_3Co$ 639.2745 (for M^+); found: 639.2740.

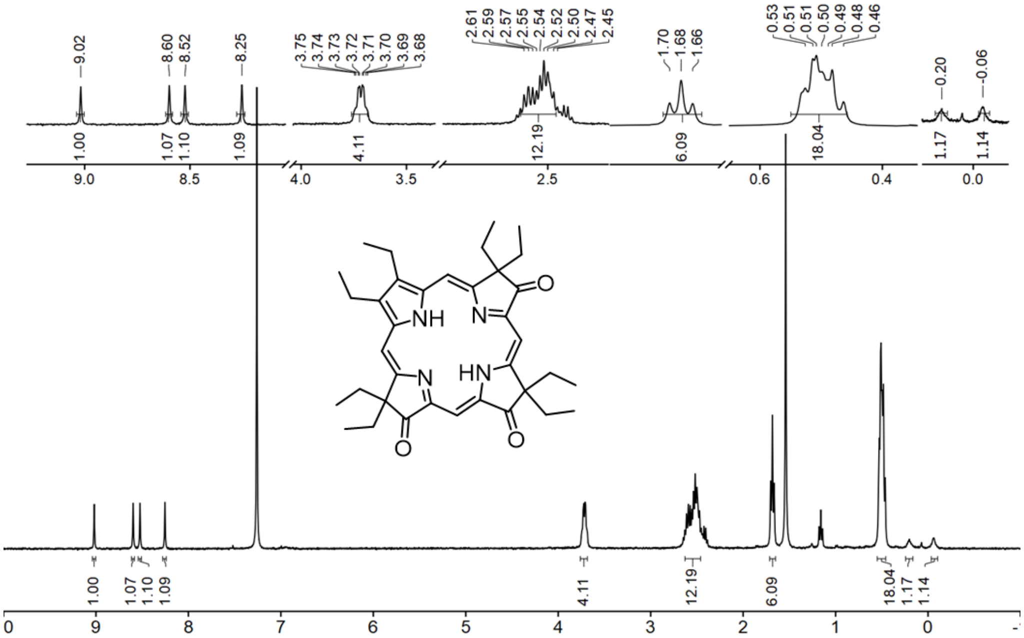

Figure S25. ^{1}H NMR spectrum (600 MHz, $CDCl_3$, 25 °C) of free-base Octaethyl-2,7,18-trioxo-pyrrocorphin (**8**).

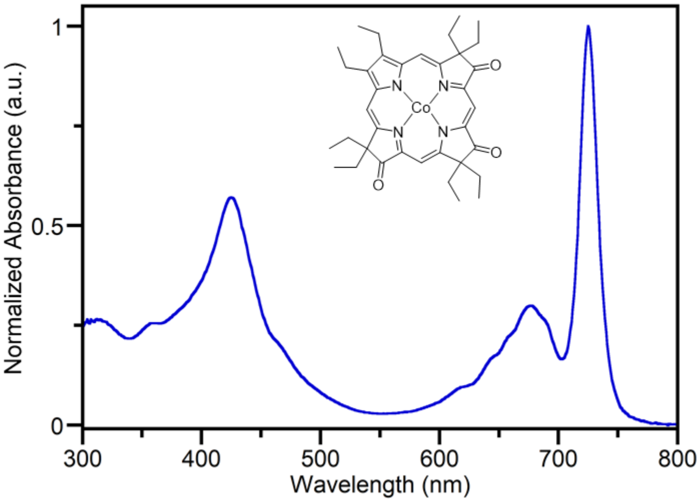

Figure S26. Normalized UV-vis spectrum (CH_2Cl_2) of **8Co**.

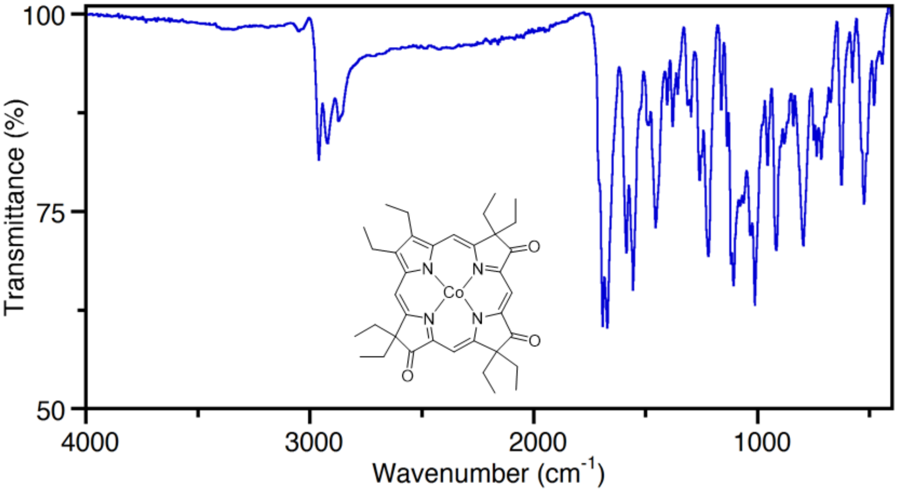

Figure S27. FT-IR spectrum (neat, ATR) of **8Co**.

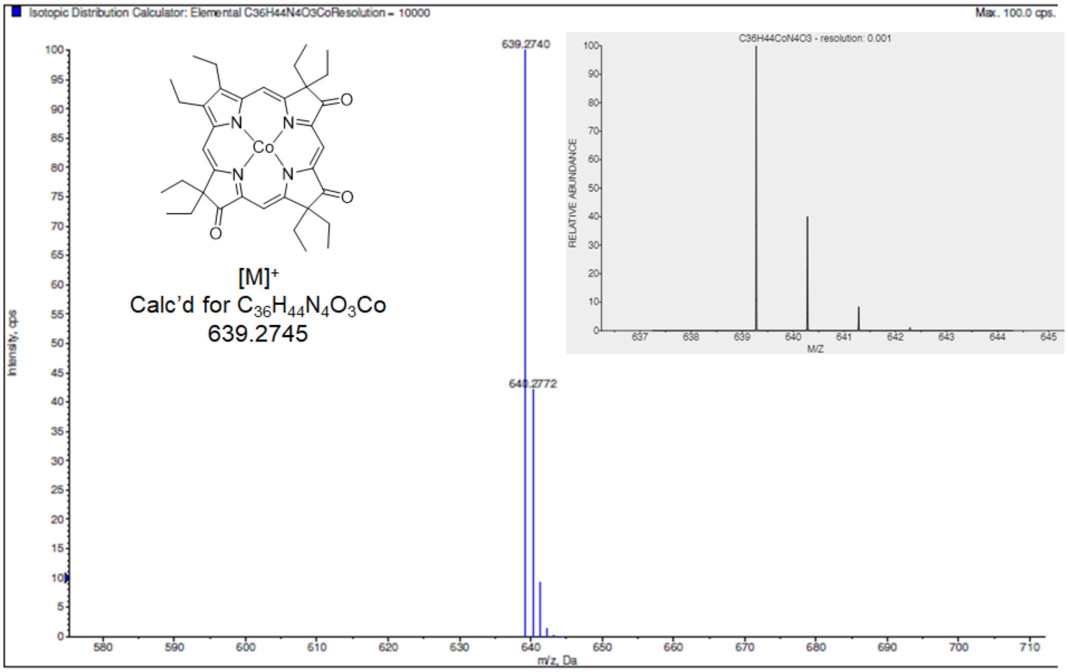

Figure S28. HR-MS (ESI+, 100% CH$_3$CN, TOF) of **8Co**.

[Octaethyl-2,7,12-trioxo-pyrrocorphinato]cobalt(II) (9Co)

Prepared in 91% yield (40 mg, 6.24 × 10^{-5} M) according to the general procedure: MW = 639.69 g/mol; R_f = 0.10 (silica-1% acetone/CH_2Cl_2); UV-vis (CH_2Cl_2) λ_{max} (log ε): 324 (4.48), 423 (4.75), 660 (4.25), 706 (4.74) nm; HR-MS (ESI+, 100% CH_3CN, TOF): *m/z* calc'd for $C_{36}H_{44}N_4O_3Co$ 639.2745 (for M^+); found: 639.2740.

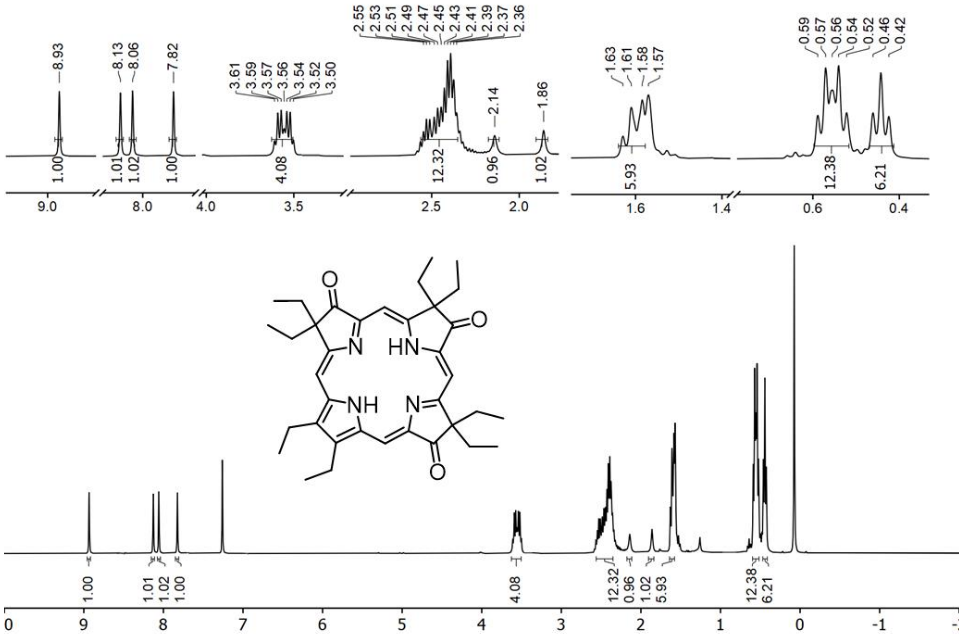

Figure S29. ^1H NMR spectrum (600 MHz, $CDCl_3$, 25 °C) of free-base Octaethyl-2,7,12-trioxo-pyrrocorphin (**9**).

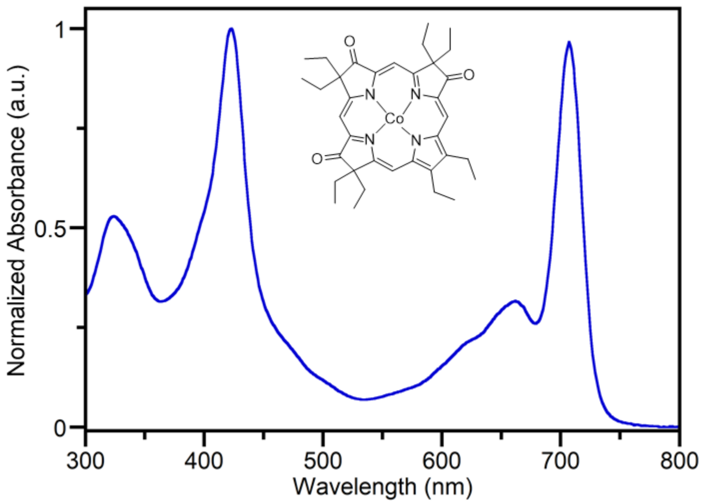

Figure S30. Normalized UV-vis spectrum (CH_2Cl_2) of **9Co**.

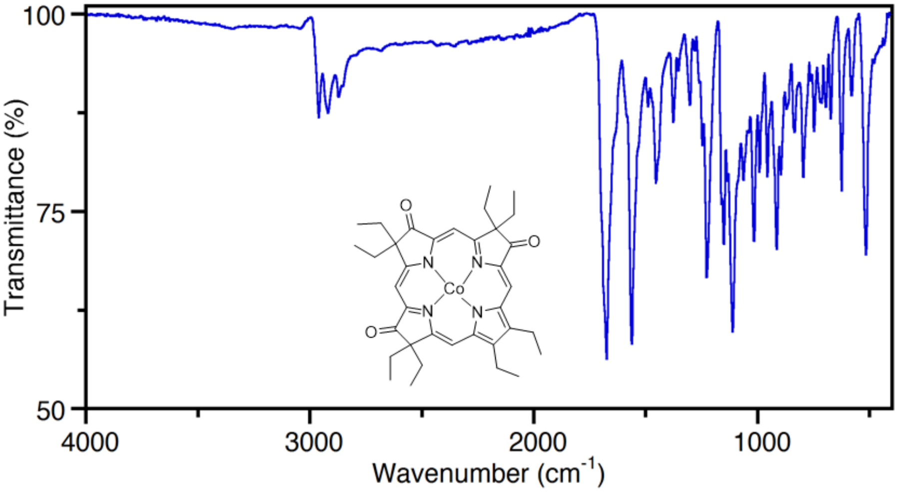

Figure S31. FT-IR spectrum (neat, ATR) of **9Co**.

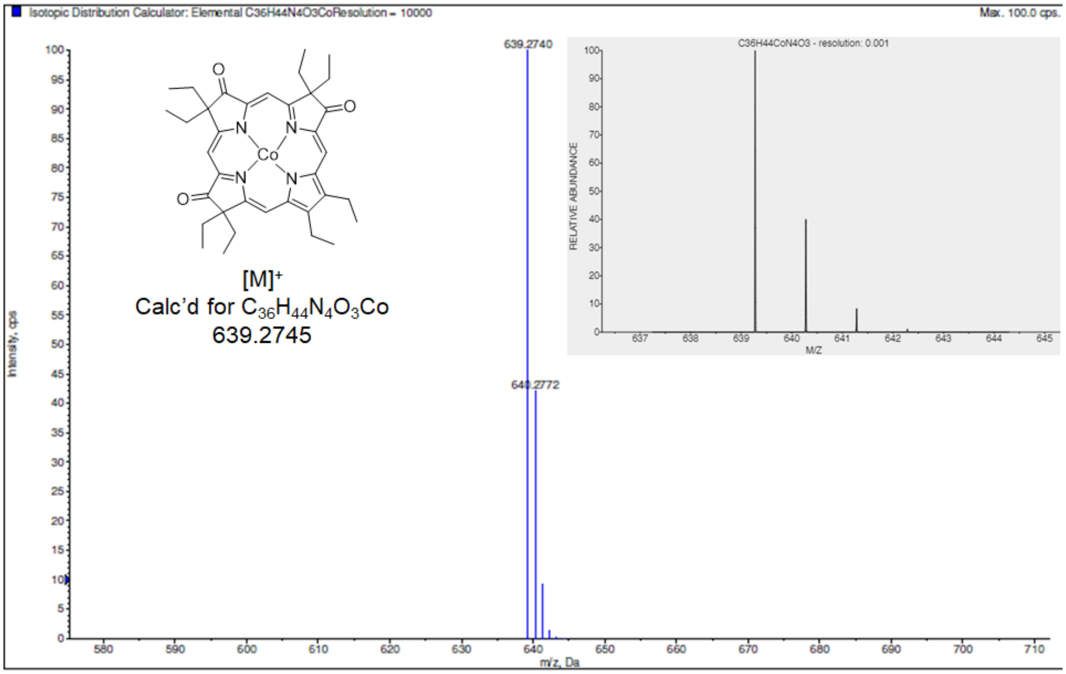

Figure S32. HR-MS spectrum (ESI+, 100% CH_3CN, TOF) of **9Co**.

Table S1: UV-vis spectral data (CH_2Cl_2, room temperature) of compounds listed

Cobalt Complexes	λ_{abs}/nm (log ε)
1Co	392 (5.32), 515 (3.97), 551 (4.31)
2Co	321 (4.19), 369 (4.47), 410 (4.88), 568 (3.82), 616 (4.42)
3Co	319 (4.39), 375 (4.44), 421 (4.76), 508 (3.50), 546 (3.38), 635 (3.71), 661 (3.92), 696 (4.92)
4Co	308 (4.26), 376 (4.37), 422 (4.53), 588 (3.93), 666 (4.42)
5Co	388 (4.36), 423 (4.30), 578 (3.80), 620 (4.26)
6Co	319 (4.06), 425 (4.56), 530 (3.47), 567 (3.64), 634 (3.60), 695 (4.38)
7Co	320 (4.12), 361 (4.20), 409 (4.48), 598 (3.72), 649 (4.31)
8Co	424 (3.93), 675 (3.65), 724 (4.17)
9Co	324 (4.48), 423 (4.75), 660 (4.25), 706 (4.74)

Electrochemical Data

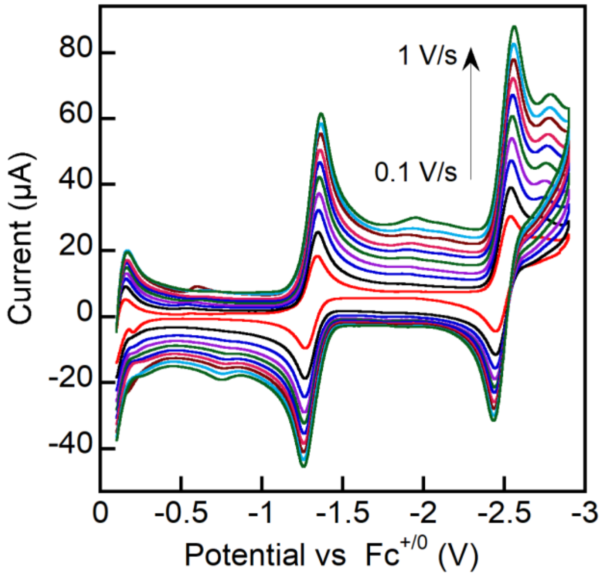

Figure S33. Cyclic voltammogram of 1mM **2Co** at different scan rates. Conditions: N_2 atmosphere, glassy carbon working electrode, platinum wire counter electrode, $Fc^{+/0}$ internal reference, scans taken at 0.1 V/s, 0.1 M [^{n}Bu$_4$N]PF$_6$, 25 °C.

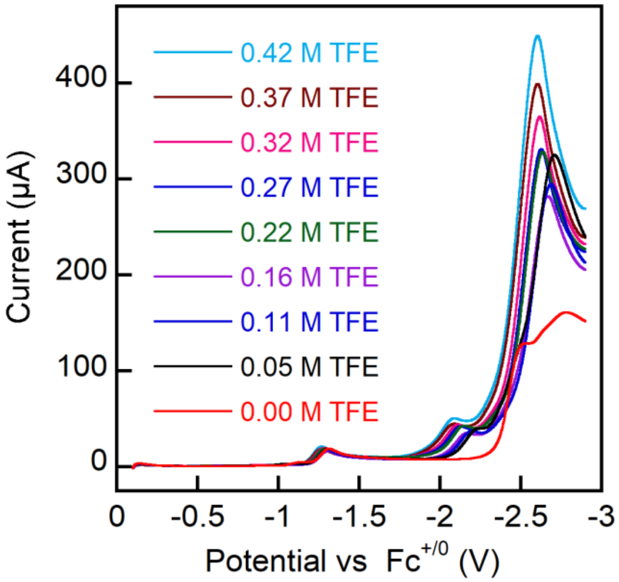

Figure S34. Cyclic voltammogram of 1 mM **2Co** at different concentrations of TFE. Conditions: CO_2 atmosphere, glassy carbon working electrode, platinum wire counter electrode, $Fc^{+/0}$ internal reference, scans taken at 0.1 V/s, 0.1 M [^{n}Bu$_4$N]PF$_6$, 25 °C.

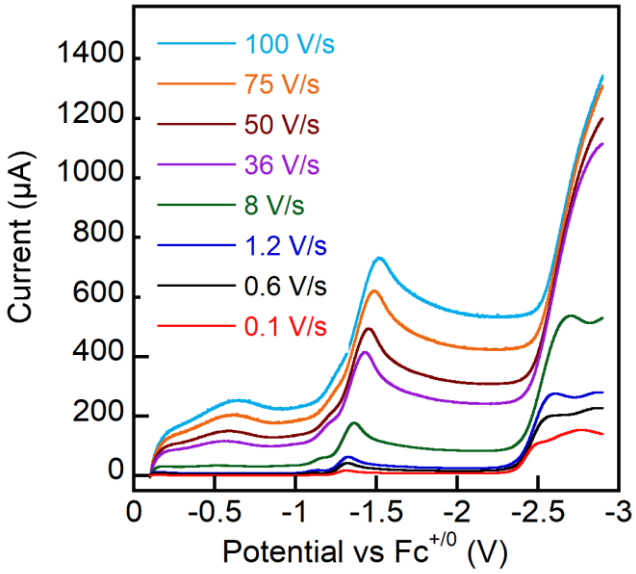

Figure S35. Cyclic voltammogram of 1 mM **2Co** at different scan rates. Conditions: CO_2 atmosphere, glassy carbon working electrode, platinum wire counter electrode, $Fc^{+/0}$ internal reference, 0.1 M [^{n}Bu$_4$N]PF$_6$, 25 °C.

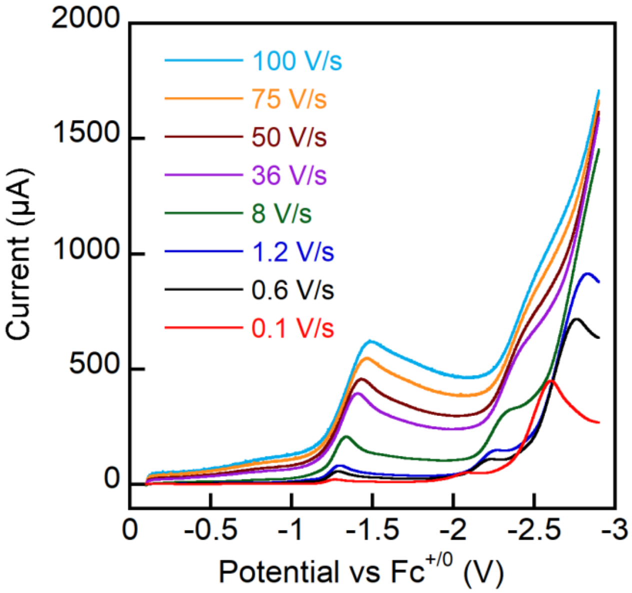

Figure S36. Cyclic voltammogram of 1mM **2Co** at different scan rates in the presence of 0.42 M TFE. Conditions: CO_2 atmosphere, glassy carbon working electrode, platinum wire counter electrode, $Fc^{+/0}$ internal reference, 0.1 M [^{n}Bu$_4$N]PF$_6$, 25 °C.

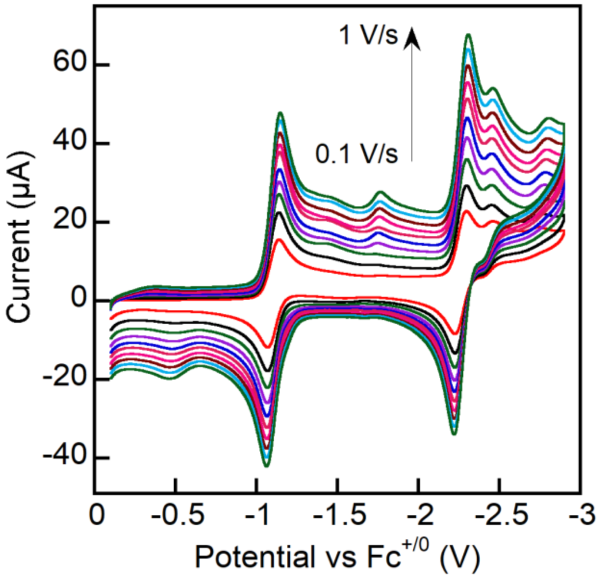

Figure S37. Cyclic voltammogram of 1mM **3Co** at different scan rates. Conditions: N_2 atmosphere, glassy carbon working electrode, platinum wire counter electrode, $Fc^{+/0}$ internal reference, scans taken at 0.1 V/s, 0.1 M $[^nBu_4N]PF_6$, 25 °C.

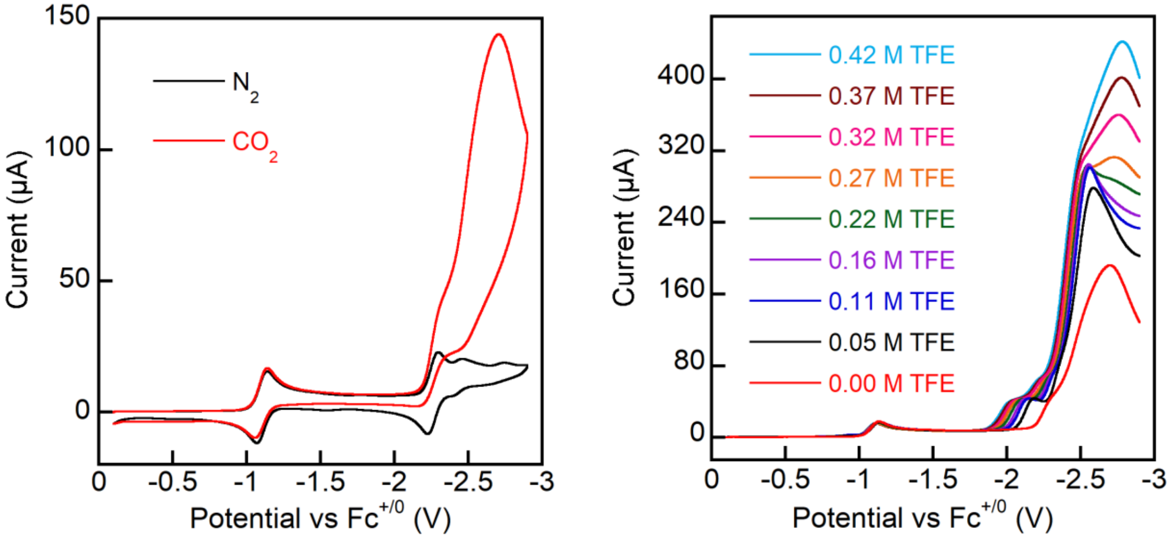

Figure S38. Cyclic voltammograms of 1mM **3Co**: (left) under N_2 atmosphere, and CO_2 atmosphere, right at different at different concentrations of TFE under a CO_2 atmosphere, Conditions: glassy carbon working electrode, platinum wire counter electrode, $Fc^{+/0}$ internal reference, scans taken at 0.1 V/s, 0.1 M $[^nBu_4N]PF_6$, 25 °C.

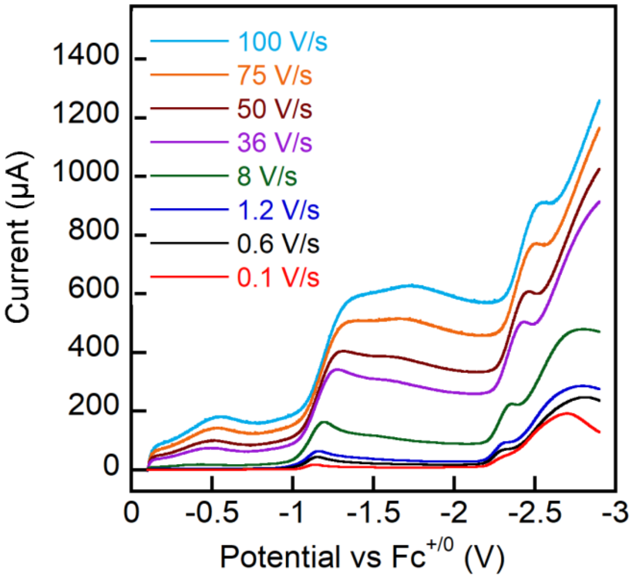

Figure S39. Cyclic voltammogram of 1mM **3Co** at different scan rates. Conditions: CO_2 atmosphere, glassy carbon working electrode, platinum wire counter electrode, $Fc^{+/0}$ internal reference, 0.1 M [$^nBu_4N$]PF_6, 25 °C.

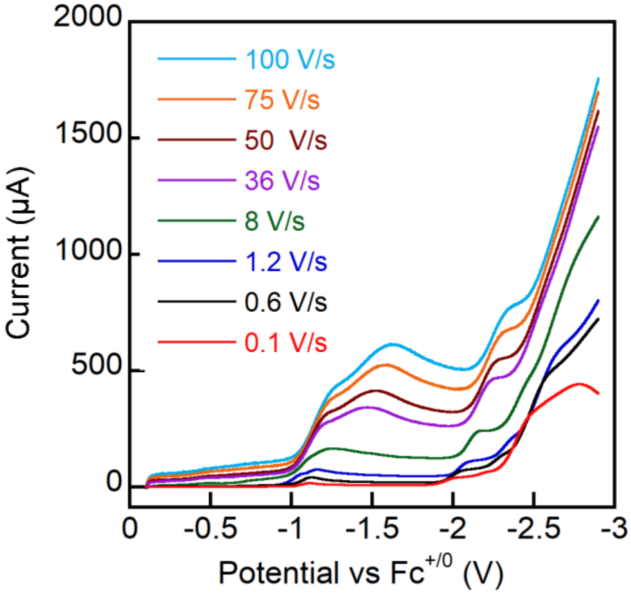

Figure S40. Cyclic voltammogram of 1mM **3Co** at different scan rates in the presence of 0.42 M TFE. Conditions: CO_2 atmosphere, glassy carbon working electrode, platinum wire counter electrode, $Fc^{+/0}$ internal reference, 0.1 M [$^nBu_4N$]PF_6, 25 °C.

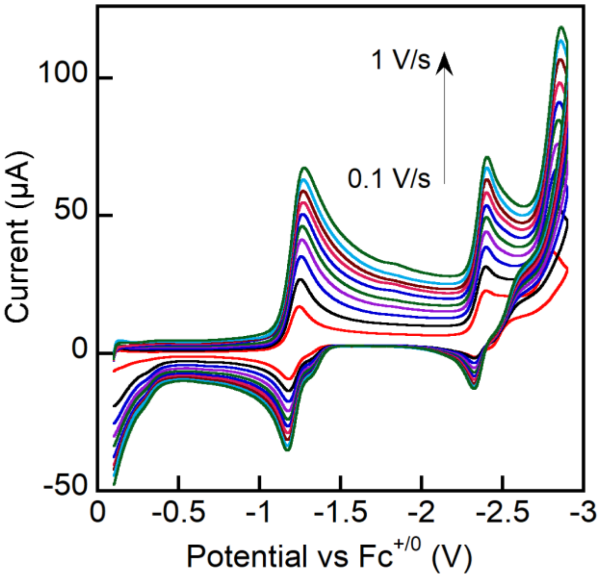

Figure S41. Cyclic voltammogram of 1mM **4Co** at different scan rates. Conditions: N_2 atmosphere, glassy carbon working electrode, platinum wire counter electrode, $Fc^{+/0}$ internal reference, scans taken at 0.1 V/s, 0.1 M [$^nBu_4N$]PF_6, 25 °C.

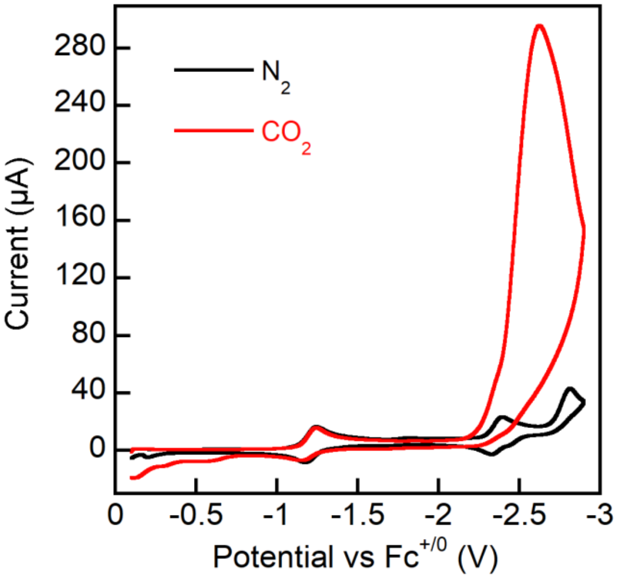

Figure S42. Cyclic voltammogram of 1mM **4Co**. Conditions: N_2 atmosphere, CO_2 atmosphere, glassy carbon working electrode, platinum wire counter electrode, $Fc^{+/0}$ internal reference, scans taken at 0.1 V/s, 0.1 M [$^nBu_4N$]PF_6, 25 °C.

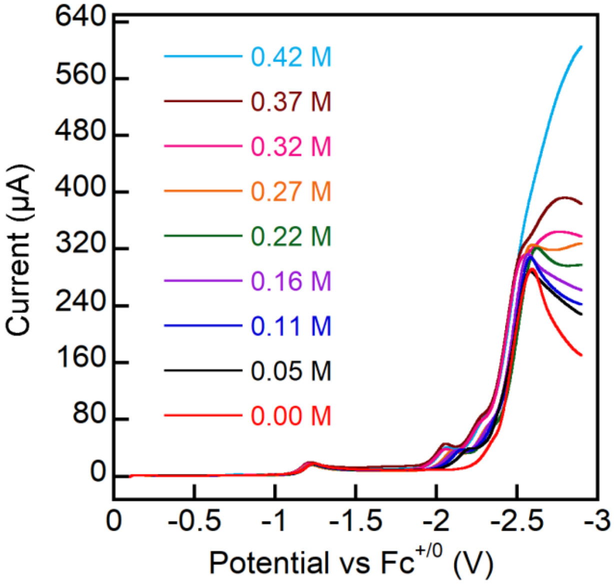

Figure S43. Cyclic voltammogram of 1mM **4Co** at different concentrations of TFE. Conditions: CO_2 atmosphere, glassy carbon working electrode, platinum wire counter electrode, $Fc^{+/0}$ internal reference, scans taken at 0.1 V/s, 0.1 M $[^nBu_4N]PF_6$, 25 °C.

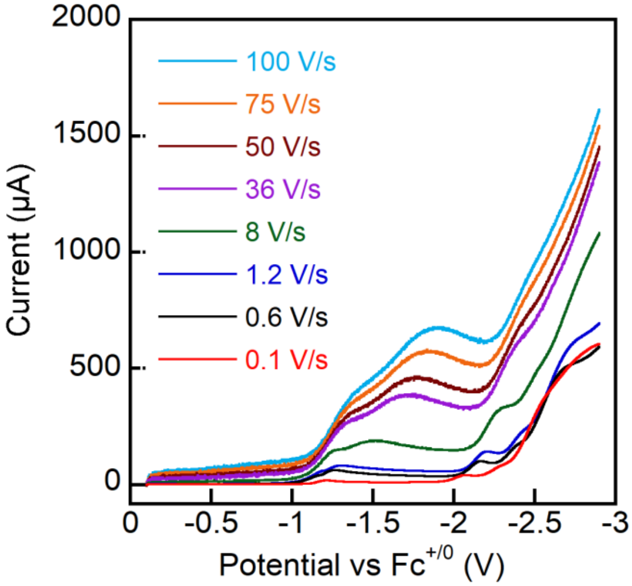

Figure S44. Cyclic voltammogram of 1mM **4Co** at different scan rates in the presence of 0.42 M TFE. Conditions: CO_2 atmosphere, glassy carbon working electrode, platinum wire counter electrode, $Fc^{+/0}$ internal reference, 0.1 M $[^nBu_4N]PF_6$, 25 °C.

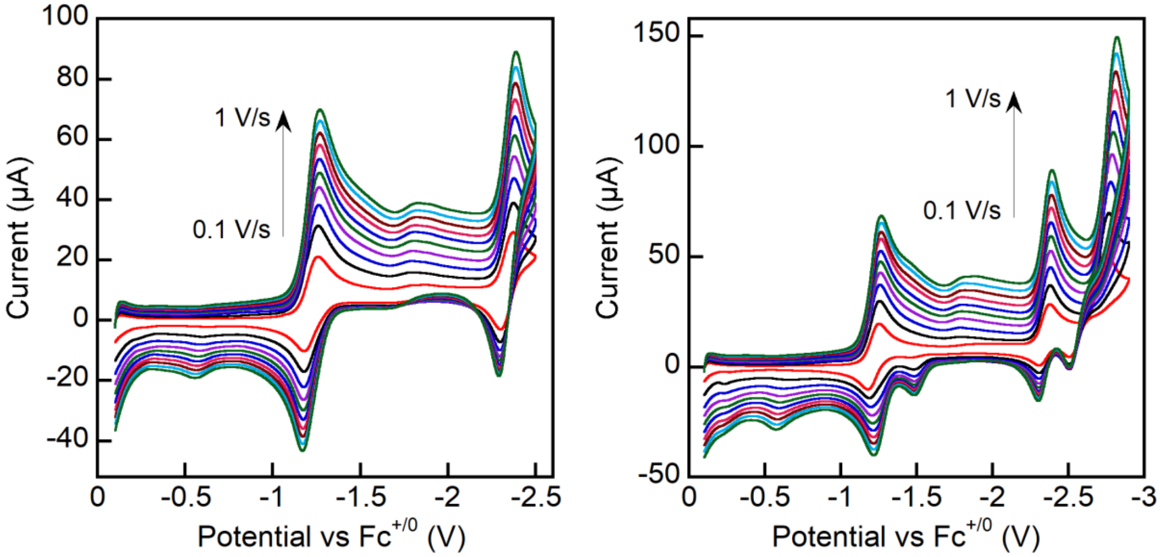

Figure S45. Cyclic voltammograms of 1mM **5Co** at different scan rates. Conditions: N_2 atmosphere, glassy carbon working electrode, platinum wire counter electrode, $Fc^{+/0}$ internal reference, scans taken at 0.1 V/s, 0.1 M $[^nBu_4N]PF_6$, 25 °C.

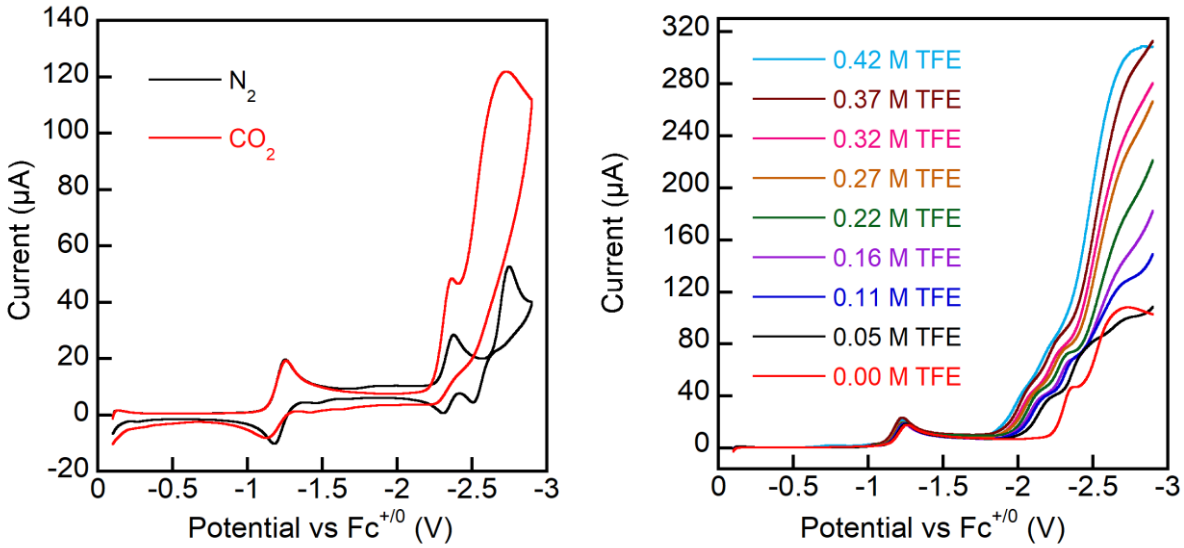

Figure S46. Cyclic voltammogram of 1mM **5Co** (left) under N_2 atmosphere, and CO_2 atmosphere, right at different at different concentrations of TFE under a CO_2 atmosphere, Conditions: glassy carbon working electrode, platinum wire counter electrode, $Fc^{+/0}$ internal reference, scans taken at 0.1 V/s, 0.1 M $[^nBu_4N]PF_6$, 25 °C.

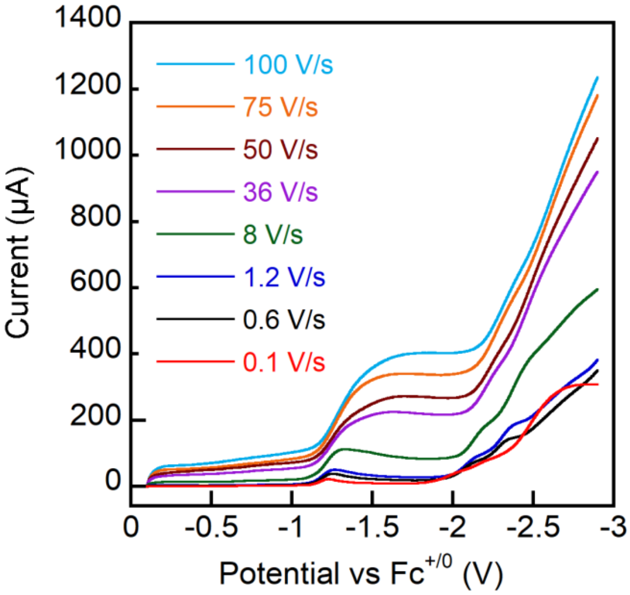

Figure S47. Cyclic voltammogram of 1 mM **5Co** at different concentrations of TFE. Conditions: CO_2 atmosphere, glassy carbon working electrode, platinum wire counter electrode, $Fc^{+/0}$ internal reference, 0.1 M [$^nBu_4N$]PF_6, 25 °C.

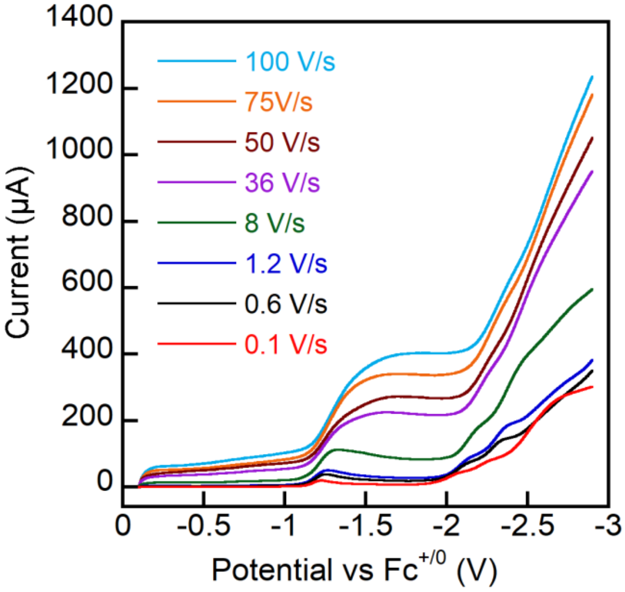

Figure S48. Cyclic voltammogram of 1 mM **5Co** at different scan rates in the presence of 0.42 M TFE. Conditions: CO_2 atmosphere, glassy carbon working electrode, platinum wire counter electrode, $Fc^{+/0}$ internal reference, 0.1 M [$^nBu_4N$]PF_6, 25 °C.

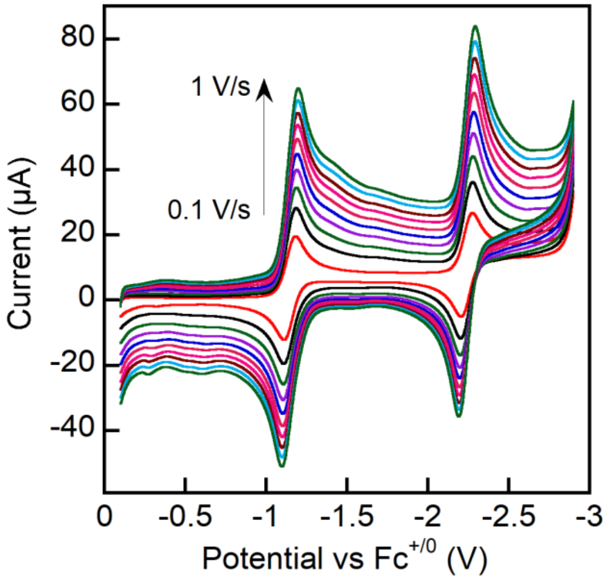

Figure S49. Cyclic voltammogram of 1 mM **6Co** at different scan rates. Conditions: N_2 atmosphere, glassy carbon working electrode, platinum wire counter electrode, Fc$^{+/0}$ internal reference, scans taken at 0.1 V/s, 0.1 M [^{n}Bu$_4$N]PF$_6$, 25 °C.

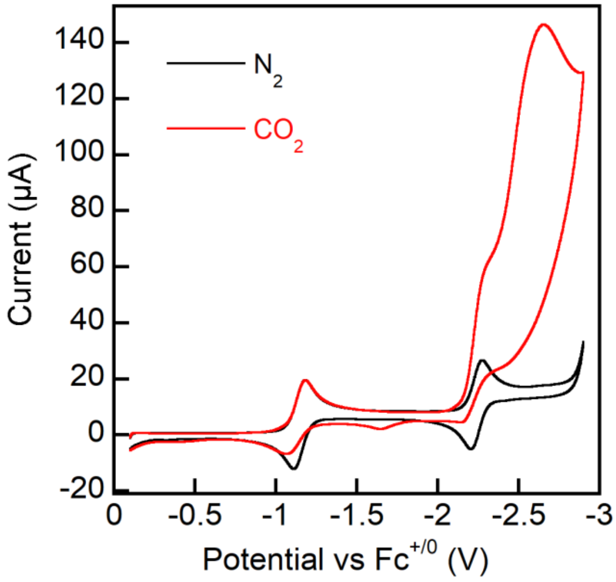

Figure S50. Cyclic voltammogram of 1 mM **6Co**. Conditions: N_2 atmosphere, CO_2 atmosphere, glassy carbon working electrode, platinum wire counter electrode, Fc$^{+/0}$ internal reference, scans taken at 0.1 V/s, 0.1 M [^{n}Bu$_4$N]PF$_6$, 25 °C.

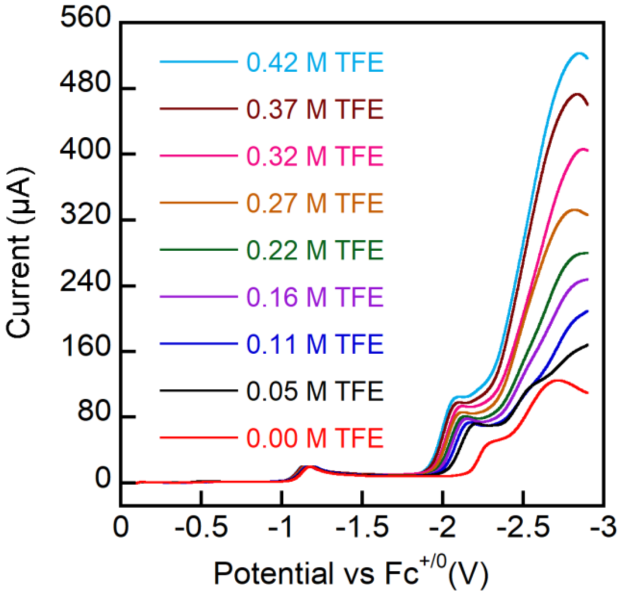

Figure S51. Cyclic voltammogram of 1 mM **6Co** at different concentrations of TFE. Conditions: CO_2 atmosphere, glassy carbon working electrode, platinum wire counter electrode, $Fc^{+/0}$ internal reference, scans taken at 0.1 V/s, 0.1 M [$^nBu_4N$]PF_6, 25 °C.

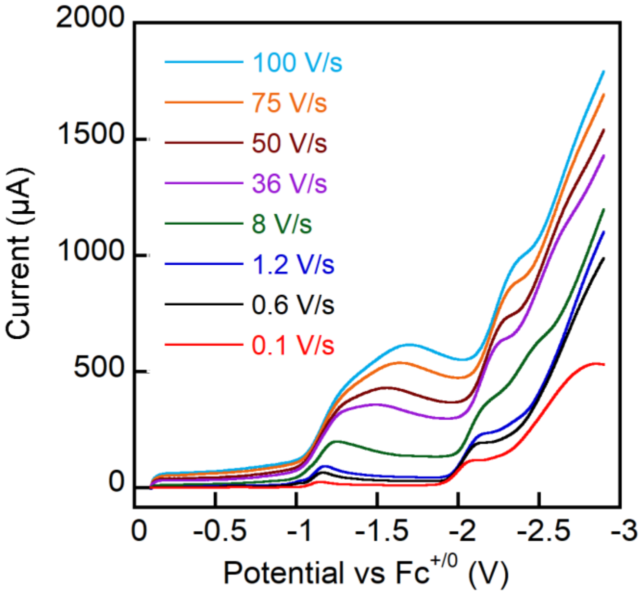

Figure S52. Cyclic voltammogram of 1 mM **6Co** at different scan rates in the presence of 0.42 M TFE. Conditions: CO_2 atmosphere, glassy carbon working electrode, platinum wire counter electrode, $Fc^{+/0}$ internal reference, 0.1 M [$^nBu_4N$]PF_6, 25 °C.

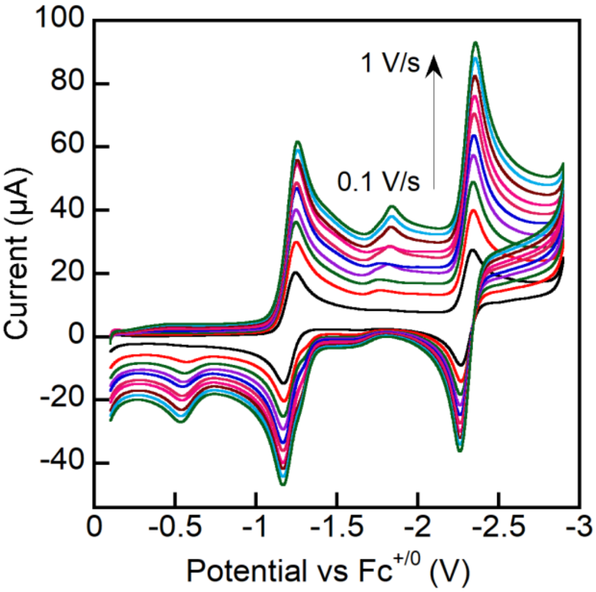

Figure S53. Cyclic voltammogram of 1mM **7Co** at different scan rates. Conditions: N_2 atmosphere, glassy carbon working electrode, platinum wire counter electrode, $Fc^{+/0}$ internal reference, scans taken at 0.1 V/s, 0.1 M $[^nBu_4N]PF_6$, 25 °C.

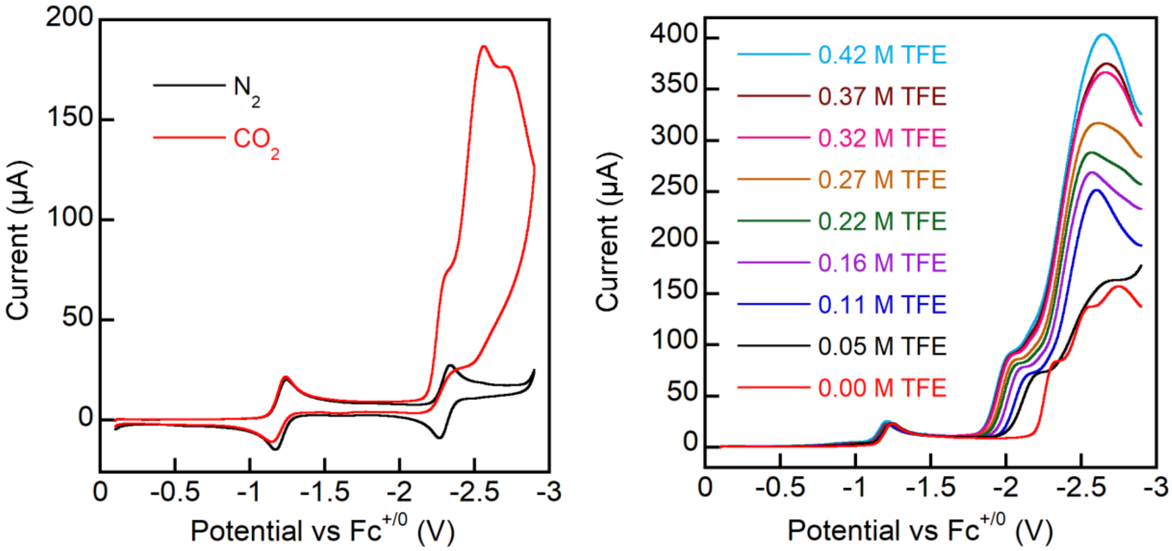

Figure S54. Cyclic voltammograms of 1mM **7Co** (left) under N_2 atmosphere, and CO_2 atmosphere, right at different concentrations of TFE under a CO_2 atmosphere. Conditions: glassy carbon working electrode, platinum wire counter electrode, $Fc^{+/0}$ internal reference, scans taken at 0.1 V/s, 0.1 M $[^nBu_4N]PF_6$, 25 °C.

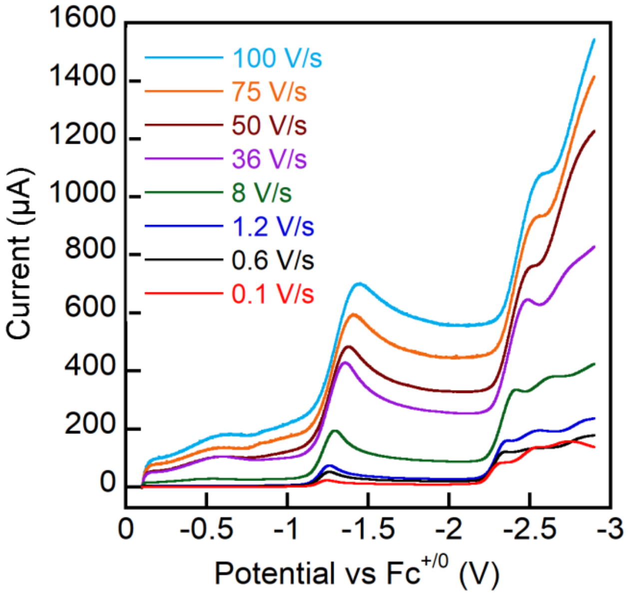

Figure S55. Cyclic voltammogram of 1mM **7Co** at different scan rates. Conditions: CO_2 atmosphere, glassy carbon working electrode, platinum wire counter electrode, $Fc^{+/0}$ internal reference, 0.1 M [$^nBu_4N$]PF_6, 25 °C.

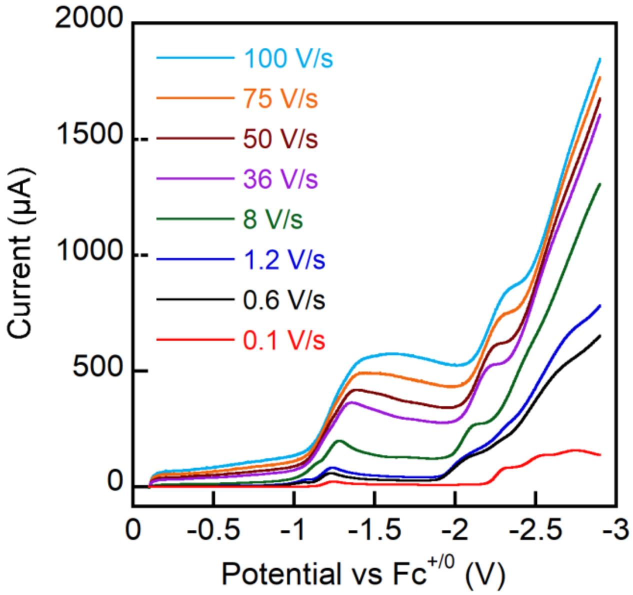

Figure S56. Cyclic voltammogram of 1 mM **7Co** at different scan rates in the presence of 0.42 M TFE. Conditions: CO_2 atmosphere, glassy carbon working electrode, platinum wire counter electrode, $Fc^{+/0}$ internal reference, 0.1 M [$^nBu_4N$]PF_6, 25 °C.

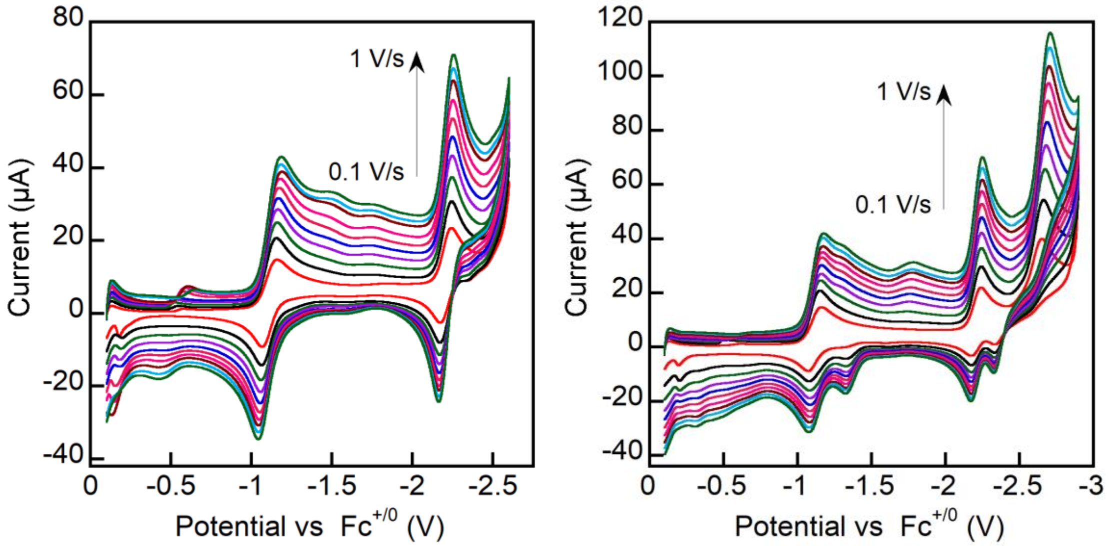

Figure S57. Cyclic voltammograms of 1 mM **8Co** at different scan rates. Conditions: N_2 atmosphere, glassy carbon working electrode, platinum wire counter electrode, $Fc^{+/0}$ internal reference, scans taken at 0.1 V/s, 0.1 M [$^nBu_4N$]PF_6, 25 °C.

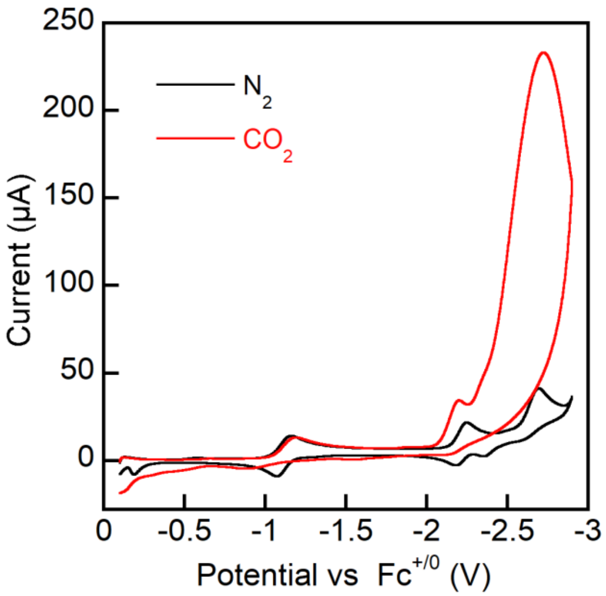

Figure S58. Cyclic voltammogram of 1 mM **8Co**. Conditions: N_2 atmosphere, CO_2 atmosphere, glassy carbon working electrode, platinum wire counter electrode, $Fc^{+/0}$ internal reference, scans taken at 0.1 V/s, 0.1 M [$^nBu_4N$]PF_6, 25 °C.

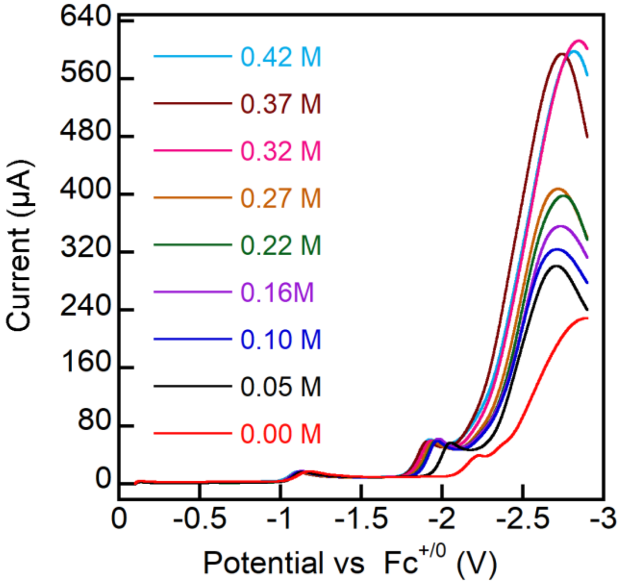

Figure S59. Cyclic voltammogram of 1 mM **8Co** at different concentrations of TFE. Conditions: CO_2 atmosphere, glassy carbon working electrode, platinum wire counter electrode, $Fc^{+/0}$ internal reference, scans taken at 0.1 V/s, 0.1 M $[^nBu_4N]PF_6$, 25 °C.

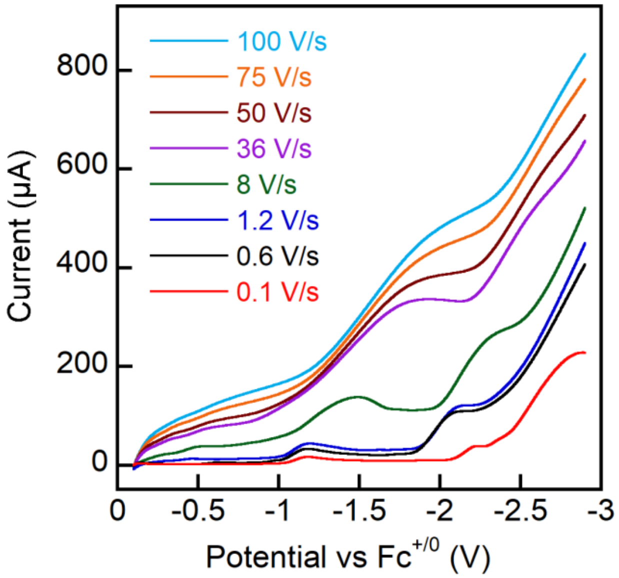

Figure S60. Cyclic voltammogram of 1 mM **8Co** at different scan rates. Conditions: CO_2 atmosphere, glassy carbon working electrode, platinum wire counter electrode, $Fc^{+/0}$ internal reference, 0.1 M $[^nBu_4N]PF_6$, 25 °C.

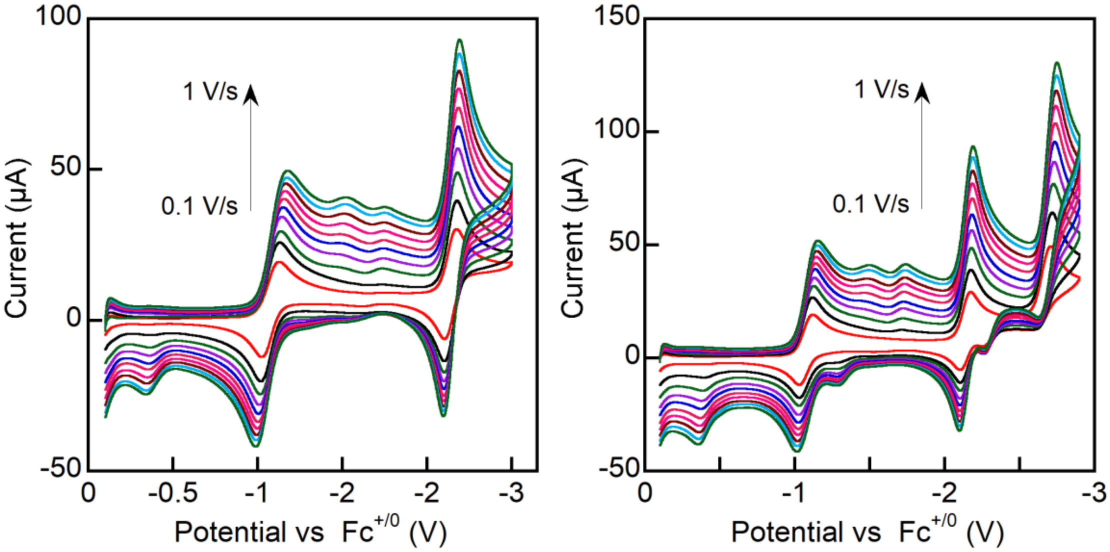

Figure S61. Cyclic voltammograms of 1 mM **9Co** at different scan rates. Conditions: N_2 atmosphere, glassy carbon working electrode, platinum wire counter electrode, Fc$^{+/0}$ internal reference, scans taken at 0.1 V/s, 0.1 M [^{n}Bu$_4$N]PF$_6$, 25 °C.

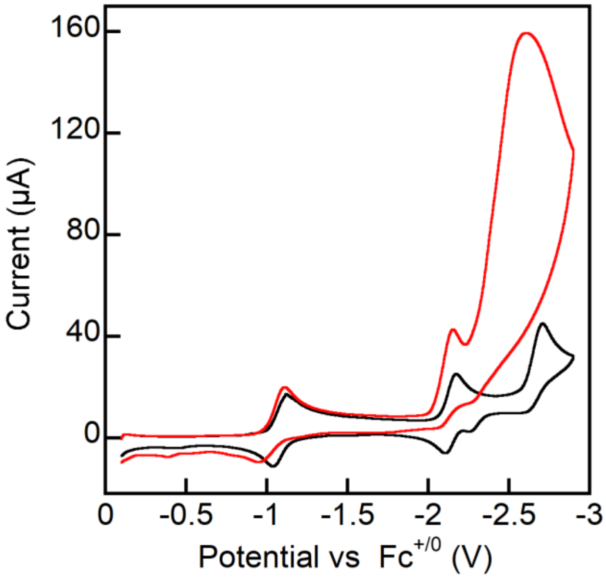

Figure S62. Cyclic voltammogram of 1mM **9Co**. Conditions: N_2 atmosphere, CO_2 atmosphere, glassy carbon working electrode, platinum wire counter electrode, Fc$^{+/0}$ internal reference, scans taken at 0.1 V/s, 0.1 M [^{n}Bu$_4$N]PF$_6$, 25 °C.

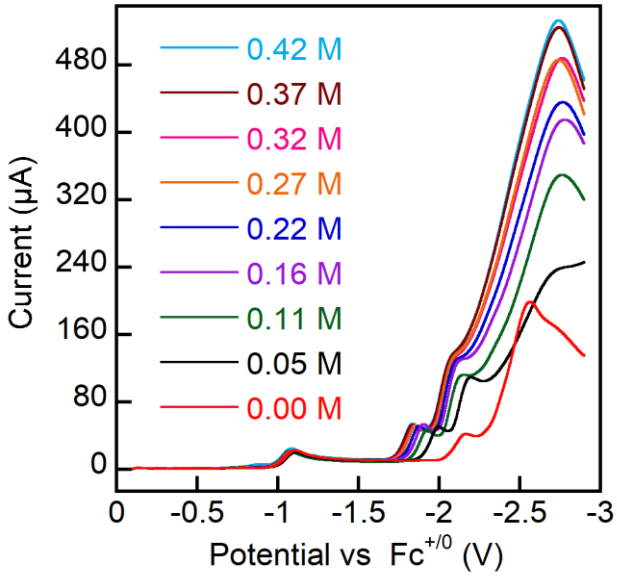

Figure S63. Cyclic voltammogram of 1 mM **9Co** at different concentrations of TFE. Conditions: CO_2 atmosphere, glassy carbon working electrode, platinum wire counter electrode, $Fc^{+/0}$ internal reference, scans taken at 0.1 V/s, 0.1 M [^{n}Bu$_4$N]PF$_6$, 25 °C.

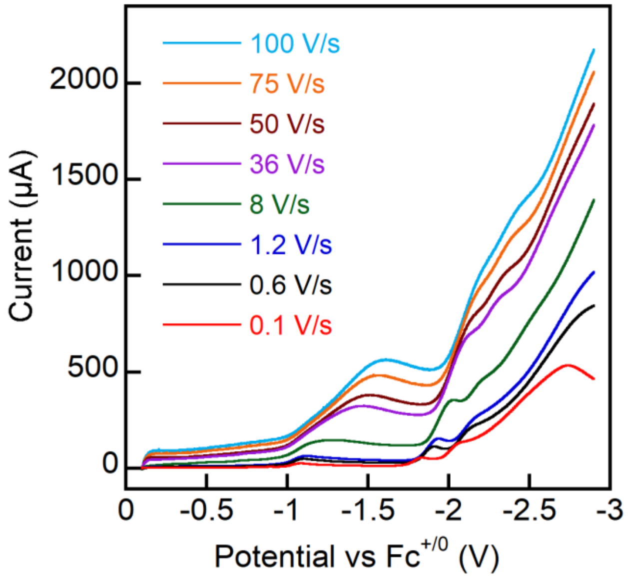

Figure S64. Cyclic voltammogram of 1 mM **9Co** at different scan rates in the presence of 0.42 M TFE. Conditions: CO_2 atmosphere, glassy carbon working electrode, platinum wire counter electrode, $Fc^{+/0}$ internal reference, 0.1 M [^{n}Bu$_4$N]PF$_6$, 25 °C.

Table S2. Summary of electrochemical results for all complexes investigated

Complex	$E_{cat/2}$ (0.00 M TFE)	$E_{cat/2}$ (0.42 M TFE)	i_{CO2}/i_{N2} (0.42 M TFE)
2Co	-2.46	-2.43	25
3Co	-2.48	-2.40	24
4Co	-2.48	-2.46	14
5Co	-2.48	-2.45	6
6Co	-2.45	-2.35	37
7Co	-2.39	-2.33	22
8Co	-2.45	-2.41	14
9Co	-2.41	-2.36	12

Table S3. Faradaic efficiencies, after CPE experiments with a glassy carbon working electrode for **2Co** held at different potentials vs $Fc^{+/0}$ as the reference for 2 hours.

Compound	Applied potential	Proton source	Faradaic efficiency (%)			
			H_2	CO	CH_4	HCOOH
2Co	-2.2	TFE	< 1	40 ± 2	-	< 1
2Co	-2.9	-	3 ± 1	59 ± 3	4 ± 2	< 3
2Co	-2.9	TFE	5 ± 1	71 ± 4	7 ± 1	< 2

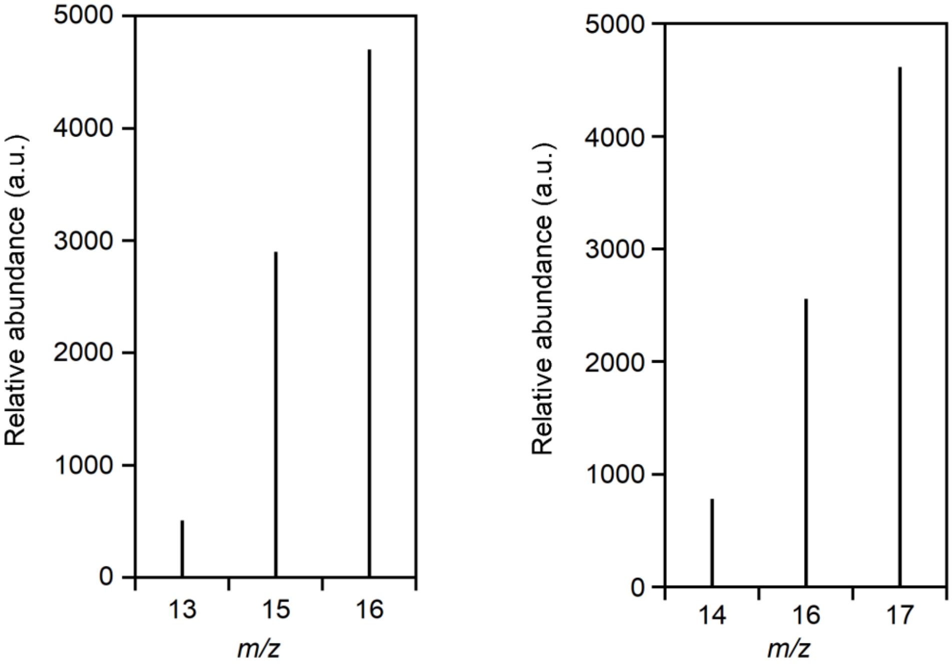

Figure S65. MS spectra of the GC-MS analysis of the CPE of **2Co** using $^{12}CO_2$ and $^{13}CO_2$ saturated in CH_3CN after controlled potential experiments for the compound **2Co** held at -2.9 V vs $Fc^{+/0}$ for 2 hours using a glassy carbon rod, a $Fc^{+/0}$ reference electrode and a platinum wire counter electrode.

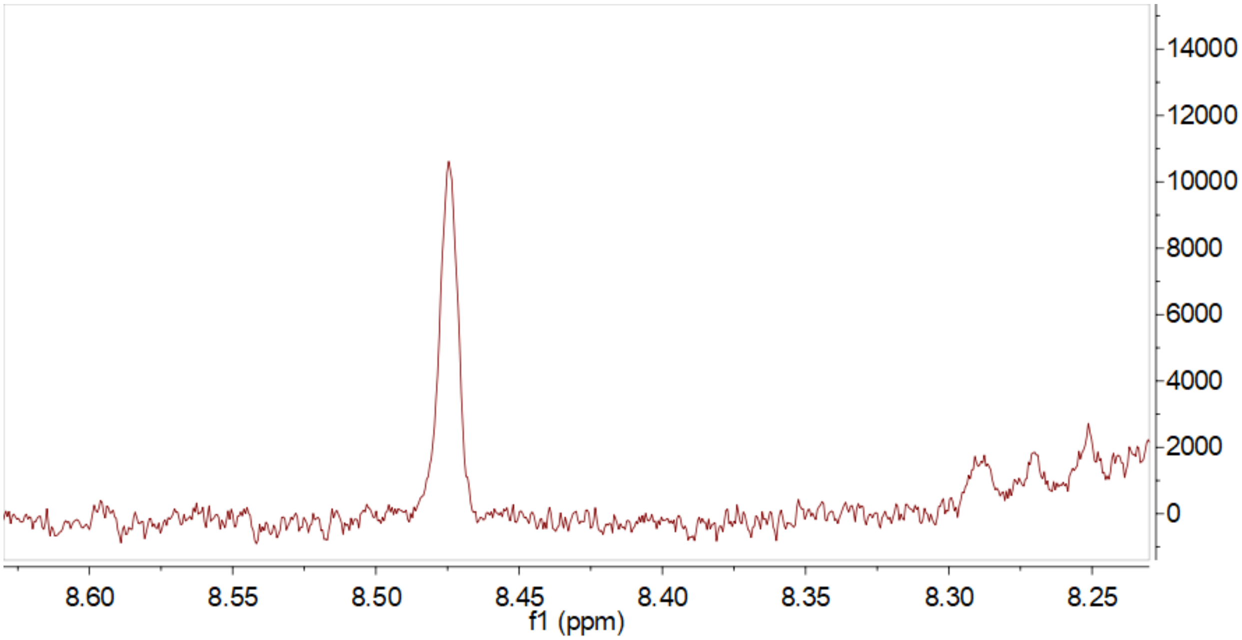

Figure S66. ^1H NMR spectrum of the controlled potential electrolysis solution of **5Co** indicating the formate chemical shift (δ = ~8.48 ppm) after workup.

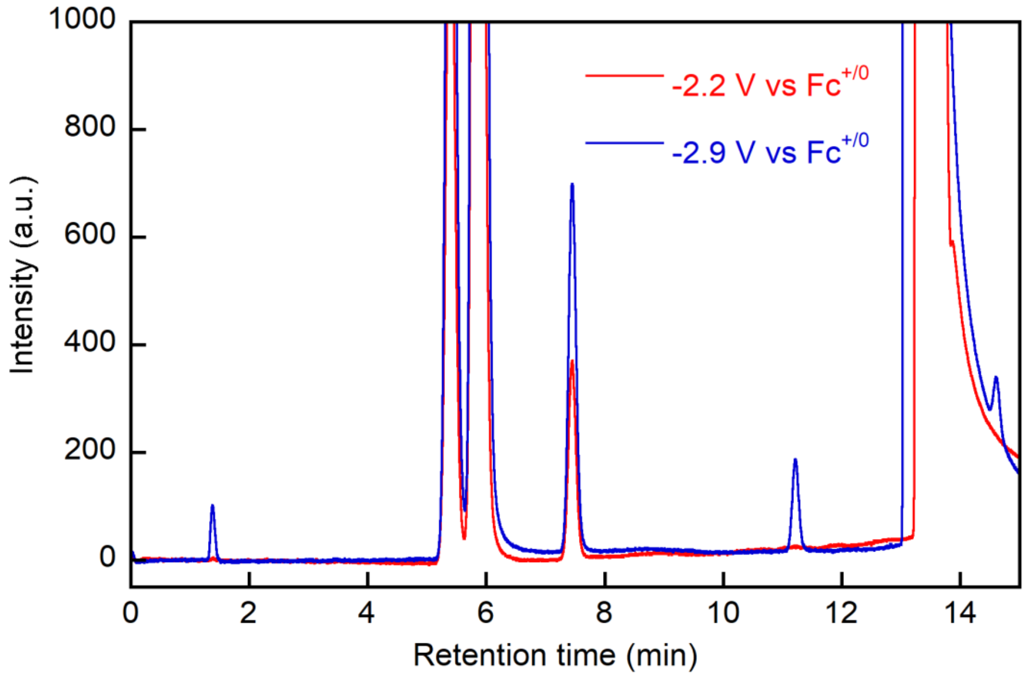

Figure S67. GC of the headspace after CPE of **2Co** in a solution of CH_3CN after bulk electrolysis experiments under an atmosphere of CO_2 held at different potentials (-2.2 V and -2.9 V vs Fc$^{+/0}$) for 2 hours (Retention peaks from left to right: H_2 (1.4 min), air (5-6 min), CO (7.5 min), CH_4 (11.3 min) and CO_2 (12.3-14.5 min)).

Table S4. Product distribution for the CO_2 Reduction by the β-Oxochlorin cobalt(II) complexes following Controlled Potential Electrolysis after 2 hrs.

Compound	C (coulombs)	H_2 (μmol)	CO (μmol)	HCOOH (μmol)	CH_4 (μmol)
2Co	21.8	3.6	70	0.6	17.6
3Co	22.5	3.2	63	0.5	15.8
4Co	21.9	3.9	77	0.7	19.9
5Co	20.8	2.9	56	0.5	14
6Co	21.5	3.5	68	0.5	17.1
7Co	19.9	3.5	67	0.6	16.9
8Co	22.3	3.1	60	0.5	15.1
9Co	21.8	3.2	62	0.5	15.5